# Farmakologia Molekularna

## Wybrane aspekty biologii strukturalnej

Andrzej Łyskowski

Cryo-EM structure of the activated GLP-1 receptor in complex with a G protein

Yan Zhang, Bingfa Sun, Dan Feng, Hongli Hu, Matthew Chu, Qianhui Qu, Jeffrey T. Tarrasch, Shane Li, Tong Sun Kobilka, Brian K. Kobilka & Georgios Skiniotis

# Publikacja

- The 2016 journal metrics for Nature are as follows:
  - 2-year Impact Factor: 40.137
  - 5-year Impact Factor: 43.769

  - The impact factor (IF) is a measure of the frequency with which the average article in a journal has been cited in a particular year. It is used to measure the importance or rank of a journal by calculating the times it's articles are cited.

  - The New England Journal of Medicine (impact factor: 72.406)
  - Chemical Reviews (impact factor: 47.928)
  - Lancet (London, England) (impact factor: 47.831)
  - Nature Reviews. Molecular Cell Biology (impact factor: 46.602)
  - …
  - Trends in Endocrinology and Metabolism (impact factor: 10.893)
  - Progress in Lipid Research (impact factor: 10.583)
  - Annual Review of Public Health (impact factor: 10.228)
  - Nucleic Acids Research (impact factor: 10.162)

# Publikacja

- Received 12 March 2016.
  - Ocena edytora
  - Ocena recnzentów
  - Poprawki
  - Ocena recenzentów

  - Decycja ostateczna
  - Edycja końcowa
- Accepted 25 April 2017.
- Published online 24 May 2017.

# Publikacja

- Abstract
- Glucagon-like peptide 1 (GLP-1) is a hormone with essential roles in regulating insulin secretion, carbohydrate metabolism and appetite. GLP-1 effects are mediated through binding to the GLP-1 receptor (GLP-1R), a class B G-protein-coupled receptor (GPCR) that signals primarily through the stimulatory G protein Gs. Class B GPCRs are important therapeutic targets; however, our understanding of their mechanism of action is limited by the lack of structural information on activated and full-length receptors. Here we report the cryo-electron microscopy structure of the peptide-activated GLP-1R–Gs complex at near atomic resolution. The peptide is clasped between the N-terminal domain and the transmembrane core of the receptor, and further stabilized by extracellular loops. Conformational changes in the transmembrane domain result in a sharp kink in the middle of transmembrane helix 6, which pivots its intracellular half outward to accommodate the α5-helix of the Ras-like domain of Gs. These results provide a structural framework for understanding class B GPCR activation through hormone binding.

## GLP-1

GLP-1 is a hormone released from the gut in response to food intake and acts on GLP-1R to stimulate glucose dependent insulin secretion from pancreatic β cells, reduce glucagon secretion from pancreatic α cells, and decrease gastric motility and appetite. Given its physiological effects, GLP-1R represents an important drug target for type 2 diabetes and obesity, with GLP-1 and its analogues already serving as approved therapeutics.

GLP-1 effects are mediated through binding to the GLP-1 receptor (GLP-1R), a class B G-protein-coupled receptor (GPCR) that signals primarily through the stimulatory G protein Gs.

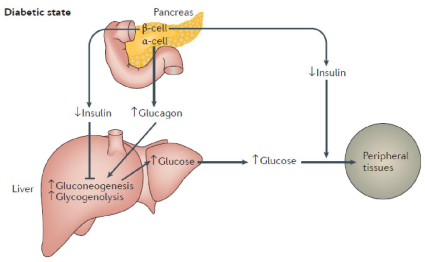


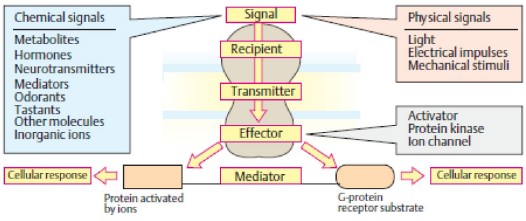

# Problem...

...lack of structural information on activated and full-length receptors.

GPCRs and their complexes have proven to be difficult targets of X-ray crystallography, often necessitating extensive engineering for conformational stabilization and crystallogenesis. Cryo-electron microscopy (cryo-EM) has recently emerged as a cutting-edge method for structure determination, yielding structures of macromolecular complexes that were otherwise unobtainable with traditional approaches.

Klasy białek:

- strukturalne
- globularne
- błonowe

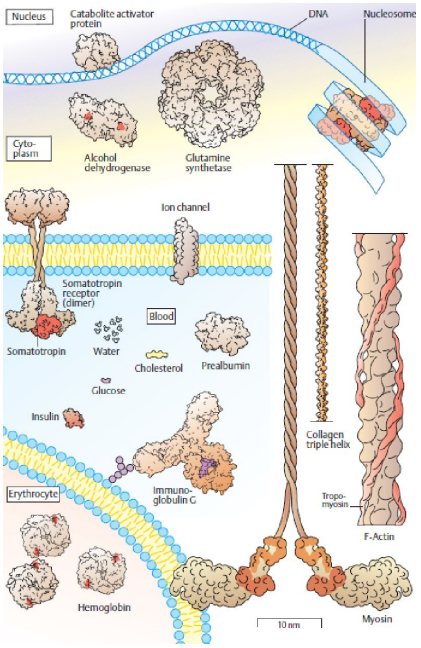


# Receptory GPCR

A large group of receptors span the membrane with α-helices seven times. These are known as 7-helix receptors. Via their effector domains, they bind and activate trimeric proteins, which in turn bind and hydrolyze GTP and are therefore called G proteins. Most G proteins, in turn, activate or inhibit enzymes that create secondary signaling molecules. Other G proteins regulate ion channels. The illustration shows the complex of the light receptor rhodopsin, with the associated G protein transducing. The GTP-binding α-subunit (green) and the γ-subunit (violet) of transducing are anchored in the membrane via lipids.

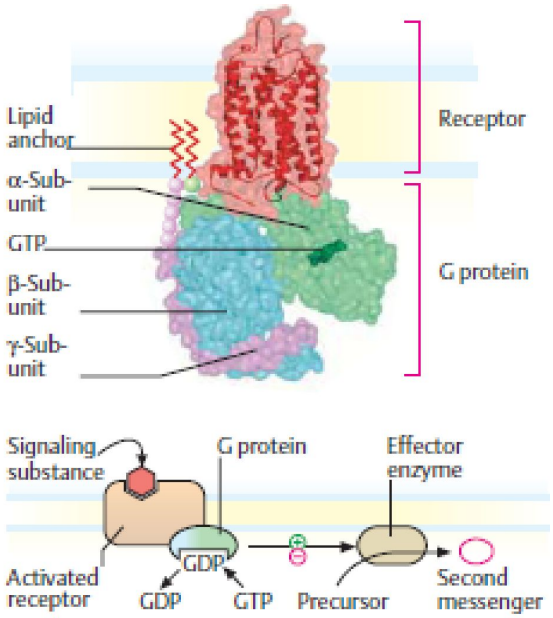

# Stabilizacja Białek

Czynniki wpływające na stabilność białek:

- oddziaływania polarne
- wodorowe
- mostki dwusiarczkowe
- kofaktory
- temperatura
- pH
- …
- środowisko

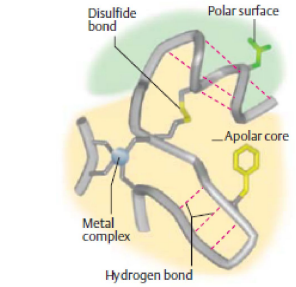


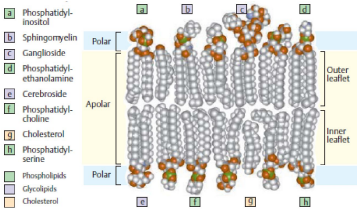


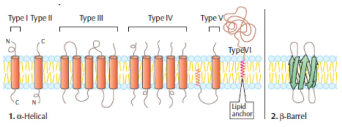


# from the low-resolution density map to the atomic coordinates

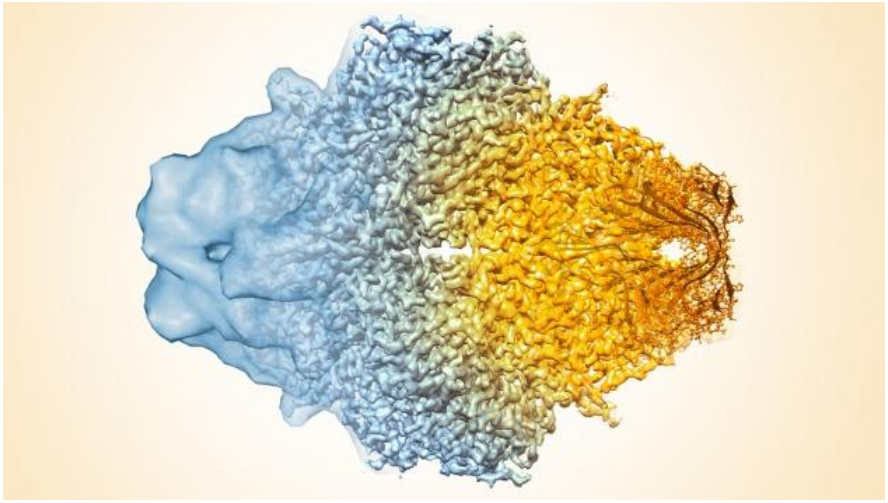

# Metody eksperymentalne

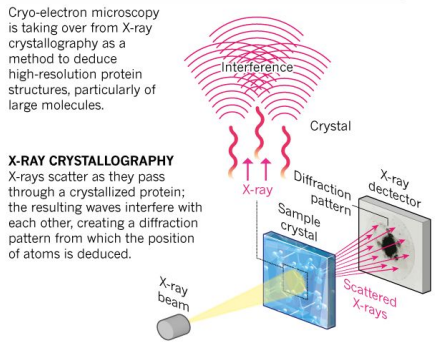


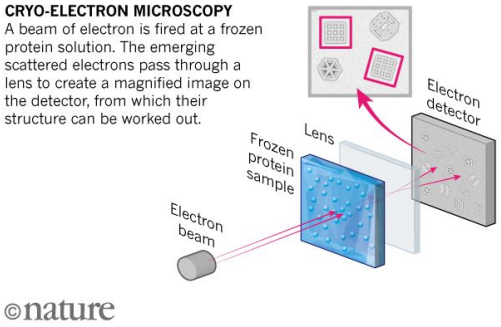


Transmission electron microscopy, as the technique is called, works more or less like ordinary microscopy, but a beam of electrons is sent through the sample instead of light. The electrons' wavelength is much shorter than that of light, so the electron microscope can make very small structures visible – even the position of individual atoms.

# Problemy

- The intense electron beam necessary for obtaining high resolution images incinerates bio-logical material and, if the beam is weakened, the image loses its contrast and becomes fuzzy.
- Electron microscopy requires a vacuum, a condition in which biomolecules deteriorate because the surrounding water evaporates.

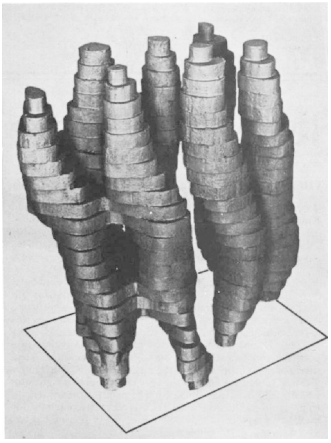

The first rough model of bacteriorhodopsin, published in 1975. Image from *Nature* 257: 28-32

It was the best picture of a protein ever generated using an electron microscope. Many people were impressed by the resolution, which was 7 Ångström (0.0000007 millimetres), but this was not enough for Richard Henderson. His goal was to achieve the same resolution as that provided by X-ray crystallography, about 3 Ångström, and he was convinced that electron microscopy had more to give.

# Procedura

1. Komputer rozpoznaje sygnał pochodzący od białek ułożonych w losowych orientacjach w przygotowanej próbce.
2. W oparciu o odpowiednie algorytmy zidentyfikowane zastają powtarzające się elementy.
3. Zebrane informacje są katalogowane i w ich oparciu powstaje model 2D.
4. Komputer generuje obraz 3D w oparciu o zebrane dane.

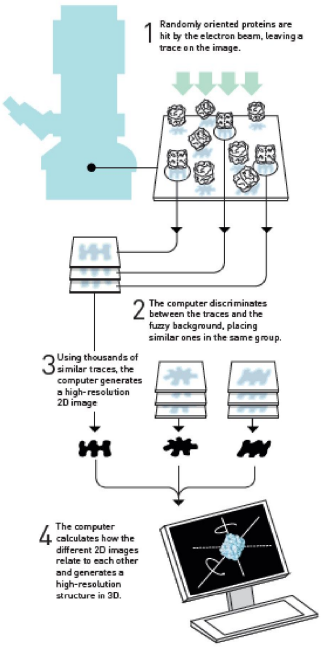

# Witryfikacja

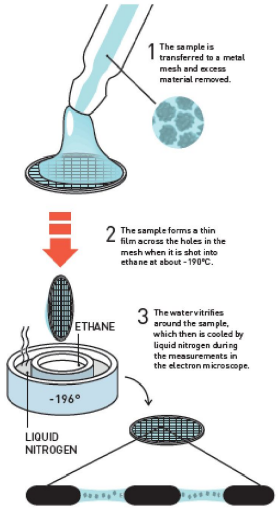


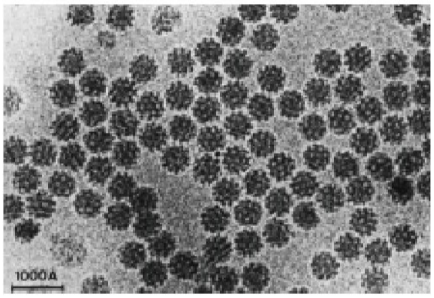


Dubochet generated the first images of viruses surrounded by vitrified water in 1984. Image from *Nature* 308: 32-36.

Initially, the research group attempted to vitrify tiny drops of water in liquid nitrogen at –196°C, but were successful only when they replaced the nitrogen with ethane that had, in turn, been cooled by liquid nitrogen. Under the microscope they saw a drop that was like nothing they had seen before. They first assumed it was ethane, but when the drop warmed slightly the molecules suddenly rearranged themselves and formed the familiar structure of an ice crystal. It was a triumph – particularly as some researchers had

# Wyznaczenie struktury

Stabilna biomolekuła

- For cryo-EM studies we used rabbit GLP-1R, which shares 92% identity with the human receptor, as it expressed at higher levels in insect cells than the human or mouse homologue.

Adekwatna stabilizacja

- GLP-1R is very unstable to extraction from membranes using conventional detergents such as DDM (n-dodecyl β-D-maltoside) and MNG (maltose-neopentyl glycol); therefore, we formed the complex between receptor and purified Gs in insect cell membranes before extraction of the GLP-1R–Gs complex with MNG and purification by antibody affinity and size-exclusion chromatography.

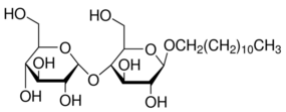


n-Dodecyl
β-D-maltoside

| | | |
|---|---|---|
| D4641-500MG | Dostępny do wysyłki 17.10.17 - Z | ~~184.50~~ 830.25 |
| D4641-1G | Dostępny do wysyłki 17.10.17 - Z | ~~268.00~~ 1,206.00 |
| D4641-5G | Tylko 5 szt. w magazynie (więcej w drodze). - Z | ~~887.00~~ 3,991.50 |
| D4641-25G | Tylko 1 szt. w magazynie (więcej w drodze). - Z | ~~3,540.00~~ 15,930.00 |

# Struktura

- Sample evaluation by negative-stain EM and single-particle averaging confirmed a monodisperse particle population and stable complex formation. Initial cryo-EM experiments suggested that the protein complex avoided areas of thin vitreous ice, and we thus had to image the specimen in relatively thick ice at the expense of increased background noise in the micrographs.

- Refinement and reconstruction of the selected particle projections after subtracting densities for the detergent micelle and the mobile α-helical domain enabled us to obtain a 3D reconstruction of the complex at 4.1 Å global resolution, with 3.9 Å nominal resolution in the core region that includes GLP-1, TMD and the α5 helix of the Gαs Ras-like domain.

# Rozdzielczość

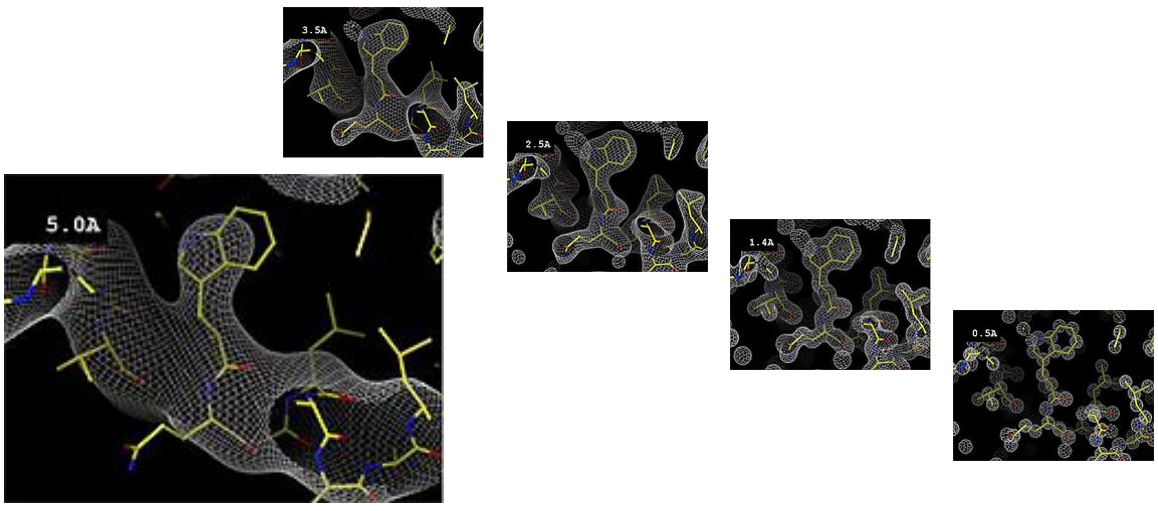

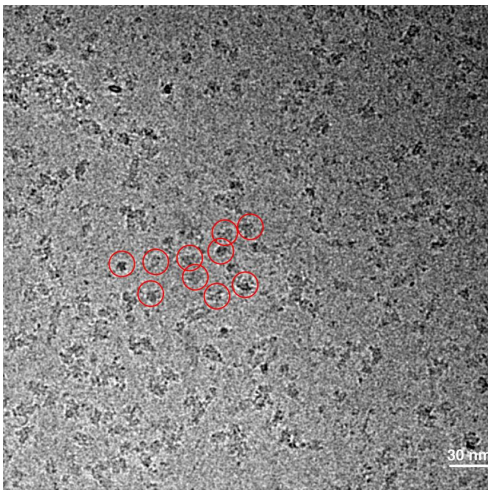


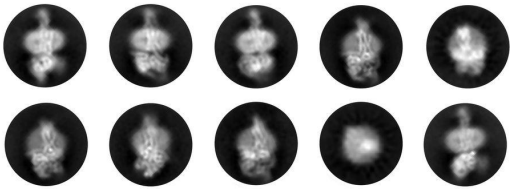

# Rekonstrukcja EM

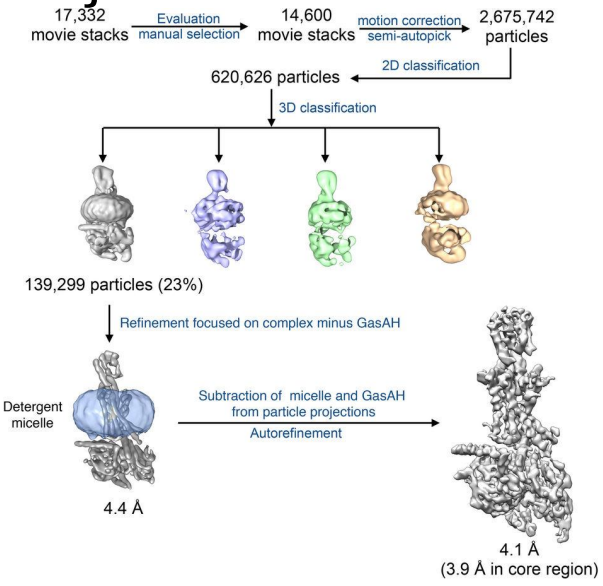

# Struktura

- Using the cryo-EM density map we built and refined a near atomic resolution structure of the GLP-1–GLP-1R–Gs complex. Side chains of primarily bulky amino acid residues are clearly identifiable in most transmembrane helices that appear to assume overall stable positions. The only exception is the cytoplasmic half of TM6, whose density is less well-defined compared to the other transmembrane helices, suggesting that this part becomes dynamic in the activated GLP-1R. The GLP-1 peptide is well-resolved, particularly in its N-terminal half that maintains interactions with the transmembrane core. This is also the case for the α5 helix of Gαs, the C-terminal part of which is stably interacting with the cytoplasmic part of GLP-1R.
- In addition, the map includes densities for all intracellular and extracellular loops (ECLs). Thus, we could resolve several key interactions of GLP-1R with GLP-1 and heterotrimeric Gs.

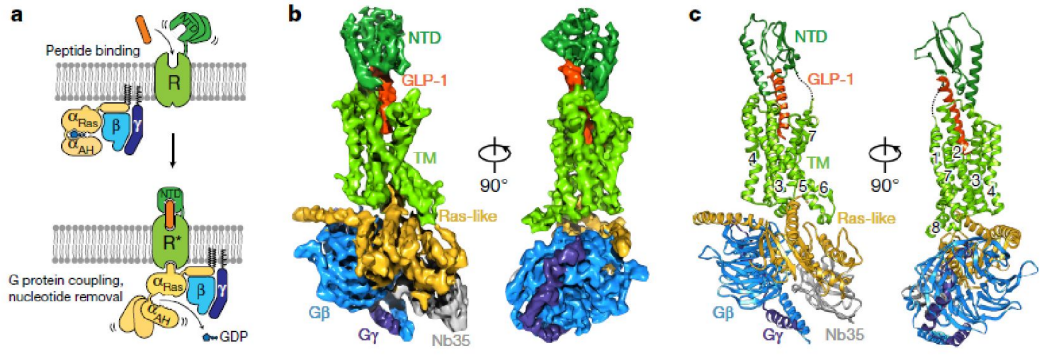


a, Schematic of the activation of a class B GPCR by extracellular peptide agonist via a ‘two-domain’ binding mechanism. AH, α-helical domain. b, Views of the GLP-1R–Gs complex cryo-EM density map, coloured by subunit (transmembrane domains in light green, NTD in dark green, GLP-1 peptide in orange, Gαs Ras-like in gold, Gβ in light blue, Gγ in dark blue and Nb35 in grey). c, Structure of the activated GLP-1R–Gs complex in the same view and colour scheme as shown in b.

# Rozpoznanie GLP-1 przez receptor
# The orthosteric peptide-binding pocket of GLP-1R

The activated GLP-1R structure shows that the GLP-1 peptide is stably anchored in its position through an extensive network of interactions that involves TM1, 2, 5, 7, ECL1 and 2, as well as the NTD.

Even though the cryo-EM map is limited in resolution, the α-helical nature of the peptide and the stability of its position have allowed us to confidently establish its main interactions with the receptor.

The interface between the C-terminal half of the peptide hormone and NTD appears identical to the one in the crystal structure of NTD–GLP-1 (Extended Data Fig. 8). Notably, the cryo-EM map suggests that the NTD is not in contact with the 7TM region, although based on our refined structure we raise the possibility of Gln213 of ECL1 interacting with Arg40 located in the α1-helix of the extracellular domain.

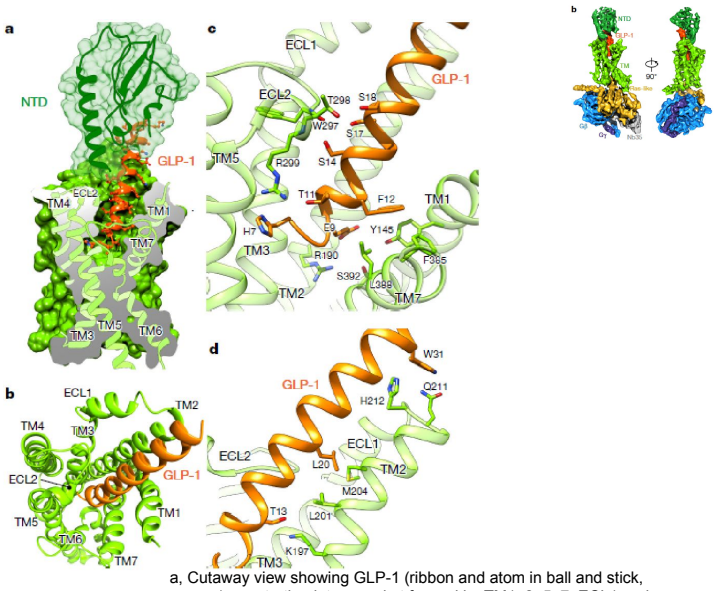


a, Cutaway view showing GLP-1 (ribbon and atom in ball and stick, orange) penetration into a pocket formed by TM1, 2, 5, 7, ECL1 and ECL2 (ribbon and surface, light green) while its C-terminal part is recognized by the NTD (ribbon in transparent surface, dark green). b, View from the extracellular side of the orthosteric peptide-binding pocket in the receptor bundle with omitted NTD. c, d, Close-up views of the interaction between the receptor and its endogenous agonist GLP-1

## Comparison of active-state GLP-1R with inactive GCGR

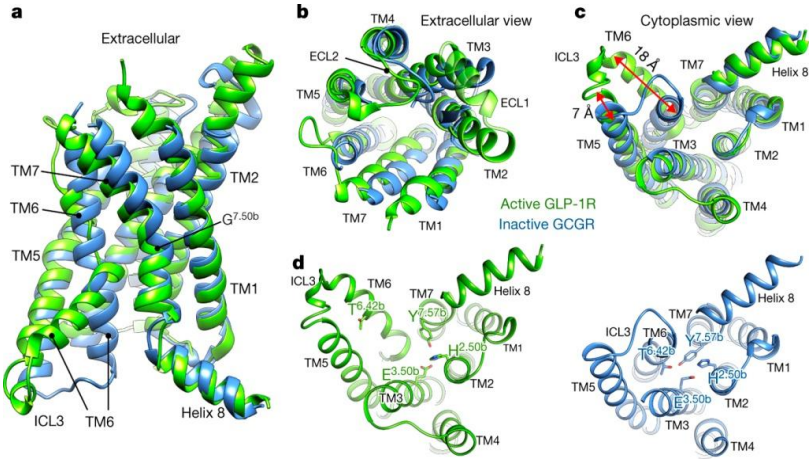


a–c, Side (a), extracellular (b) and cytoplasmic (c) views of the activated GLP-1R transmembrane bundle (light green) in superposition to the inactive glucagon receptor bound to allosteric antagonist (not shown; PDB code: 5EE7, blue). Significant conformational changes are observed on the cytoplasmic face of TM5 and TM6. TM6 moves outwards by 18 Å as measured at the Cα of Lys346, while TM5 moves a smaller distance by 7 Å when measured at the Cα of Lys334. A notable difference on the extracellular side is TM2 extended by three helical turns stabilized by peptide ligand binding. The disordered extracellular loops in the inactive GCGR structure are stabilized and structurally ordered in the activated GLP-1R structure. d, Comparison of HETX motif networking (in stick representation, Wootten numbering in superscript) between inactive GCGR and active GLP-1R shows that the outwards movement of TM6 removes T6.42b from the polar network.

## Polar network rearrangements upon GLP-1R activation

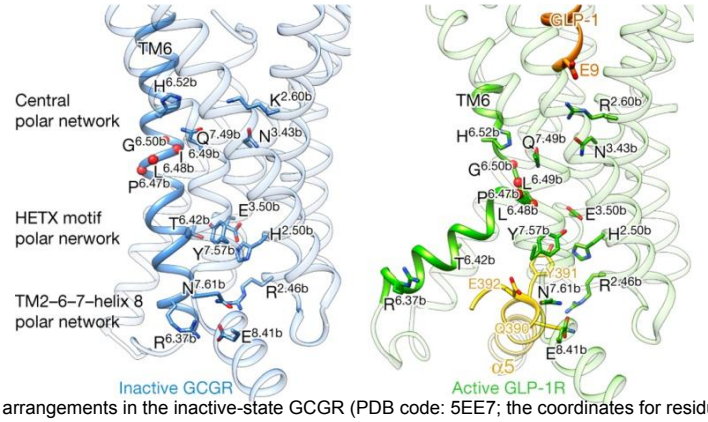


Comparison of polar network arrangements in the inactive-state GCGR (PDB code: 5EE7; the coordinates for residue R2.46b were obtained from the crystal structure of apo GCGR) and active-state GLP-1R. GLP-1 binding results in an outward movement of the cytoplasmic half of TM6 with simultaneous rearrangements of the central polar network. The rearrangement of TM6 breaks apart polar interactions of the conserved HETX and TM2–6–7–helix 8 networks, releasing residues for interactions with the α5-helix of the Gαs Ras-like domain. Peptide ligand GLP-1, TM6 and the α5-helix of Gαs Ras-like are shown in ribbon representation and coloured as in Fig. 1. Polar network residues are shown in stick representation with Wootten numbering in superscript. The exposed backbone carbonyl oxygen atoms of Pro6.47b-Leu-Leu-Gly6.50b are shown as red spheres.

## GLP-1R interactions with $G_s$

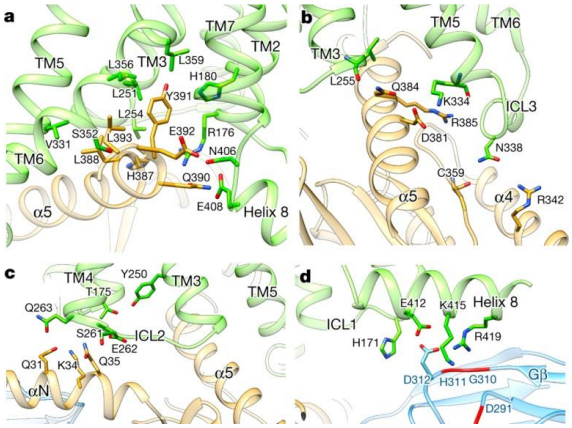


a, b, The α5-helix of the Gαs Ras-like domain docks into a cavity on the intracellular side of the receptor transmembrane bundle formed by the opening of transmembrane helices 5 and 6. a, Gs interactions with the transmembrane core include polar and non-polar contacts. The recognition of Y391 of the α5-helix involves both a small hydrophobic pocket formed by L251, L356 and L359, and potential hydrogen bonding with H180 of the conserved polar network, equivalent to the E/DRY motif in class A GPCRs. b, Q384 and R385 of the α5-helix form a polar interaction network with the cytoplasmic ends of TM3 and TM5, respectively. N338 of ICL3 is in close proximity to R342 of the α4-helix and C359 of the β4-strand. c, Y250 of TM3 and T175 of TM2 form a hydrogen bond constraining the conformation of ICL1 and ICL2 with respect to each other. E262 and Q263 at the intracellular tip of TM4 and S261 of ICL2 form polar interactions with the stretch Q31–Q35 of αN-helix. d, H171 of ICL1 participates in the electrostatic interaction network between E412, K415 and R419 of helix 8 with D312 and D291

Crystal structure of the GLP-1 receptor bound to a peptide agonist

Ali Jazayeri, Mathieu Rappas, Alastair J. H. Brown, James Kean, James c. Errey, Nathan J. Robertson, Cédric Fiez-Vandal, Stephen P. Andrews, Miles Congreve, Andrea Bortolato, Jonathan S. Mason, Asma H. Baig, Iryna Teobald, Andrew S. Doré, Malcolm Weir, Robert M. Cooke & Fiona H. Marshall

ARTYKUŁ

Received 10 February; accepted 9 May 2017.
Published online 31 May 2017.

**Extended Data Table 2 | Data collection and refinement statistics for GLP-1R StaR complexed with peptide 5**

| | |
|---|---|
| **Data collection** | |
| Number of crystals | 8 |
| Space group | $P3_121$ |
| Cell dimensions | |
| a, b, c (Å) | 94.44, 94.44, 163.9 |
| α, β, γ (°) | 90, 90, 120 |
| Number of reflections measured | 60,956 |
| Number of unique reflections | 9,266 |
| Resolution (Å) | 54.63 – 3.7 (4.05 – 3.70) |
| $R_{merge}$ | 0.134 (2.024) |
| $R_{pim}$ | 0.073 (1.078) |
| $CC_{1/2}$** | 0.998 (0.348) |
| Mean I/sd(I) | 5.6 (1.2) |
| Completeness (%) | 98.5 (99.7) |
| Redundancy | 5.6 (6.9) |
| **Refinement** | |
| Resolution (Å) | 24.677 – 3.70 |
| Number of reflections (test set) | 16,091 (763) |
| Reflection test set (%) | 4.74 |
| $R_{work}/R_{free}$ | 0.285 / 0.334 |
| Number of atoms | |
| All | 3,409 |
| Protein | 3,242 |
| Ligand | 107 |
| Others (Lipids, ions, waters) | 60 |
| Average B factors (Å$^2$) | |
| All | 180.8 |
| GLP1R | 181.0 |
| Ligand | 166.0 |
| Others (detergent, sugars) | 190.9 |
| RMSD | |
| Bond lengths (Å) | 0.004 |
| Bond angles (°) | 1.021 |
| Ramachandran statistics | |
| Favoured regions (%) | 96.38 |
| Allowed regions (%) | 3.62 |
| Outliers (%) | 0.0 |
| *MolProbity* overall score | 2.13 (100$^{th}$ percentile) |

Values in parentheses indicate highest resolution shell. **$CC_{1/2}$, see ref. 47.

XRD

1. Protein crystallization.
2. Crystal harvesting.
3. Data collection and processing.
4. Data analysis.
5. Structure refinement and analysis.

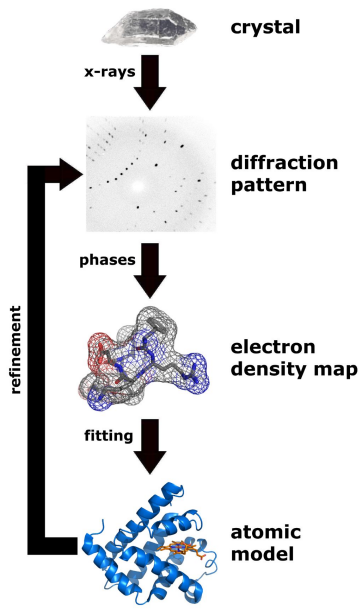


By Thomas Splettstoesser (www.scistyle.com) - own work; the public domain image Myoglobindiffraction.png [1] was used; the other images were rendered with PyMol (www.pymol.org) based on PDB id 1MBO, CC BY-SA 3.0,

# PROTEIN CRYSTALLIZATION

## The First Protein Crystal & Beyond

The first record of crystals of biological macromolecules were those of hemoglobin, reported by Hunefeld around 1840. During the 1880s, crystallization moved from being a mere curiosity to a method for purification. During the 1920s and 1930s crystallization grew in popularity, with the crystallization of insulin by John Jacob Abel and colleagues, as well as work by James B. Sumner, demonstrating enzymes could be obtained as crystalline proteins, alongside the work with a number of important crystalline enzymes by John Northrop and colleagues. It was not until the late 1930s that crystalline proteins were introduced to X-rays, beginning a torrid affair that shines bright to this day.

Much has changed with how biological macromolecules are sourced. Early on, and to a small extent today, samples were obtained by protein chemists through extraction and purification from natural sources, including plants, as well as various organs and tissues of pigs, cows, and other animals. In the 1980s, with the near cataclysmic death of heavy metal and the fortuitous end of disco, geneticists and molecular biologist rose above the fog and hair spray, allowing DNA technology to integrate with structural biology, totally accelerating and transforming the field of structural biology.

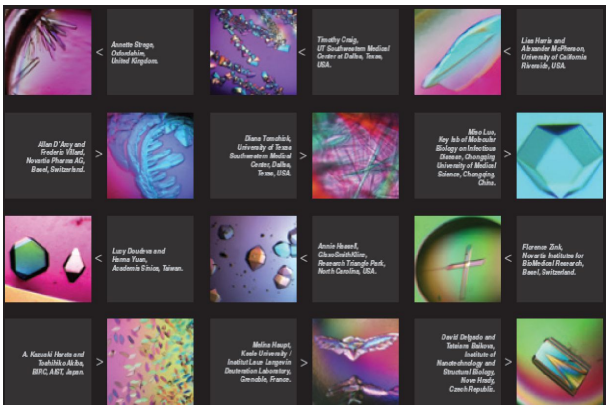


# PROTEIN CRYSTALLIZATION

## It's Simple, But Complicated

Although much change, and the numerous advancements in molecular biology and crystallography has reduced many of the arduous, laborious, math and physics infused tasks to, in some cases, the mere push of a button, crystallization remains at the crossroads where science meets art. The growth and optimization of crystals of biological macromolecules remains largely empirical in nature. There is no comprehensive theory to guide efforts and experiments related to the crystallization of proteins, nucleic acids, and other biological macromolecules. Although much knowledge and experience has been accumulated, the crystallization of a protein involves collected wisdom, intuition, creativity, patience, and perseverance.

Crystallization of biological macromolecules composed of many thousands of different atoms, bound together with many degrees of freedom, is a complex task. Confounding this many variables and factors influencing the crystallization experiment.

This extensive number of variables confounded with typically limited sample material negates a precise and reasoned strategy typically applied to a scientific problem. Instead, crystallization is often a matter of searching, as systematically as possible, through crystallization experiments, to identify those variables key to success, as well as their ranges. Initially, one employs crystallization screening, typically to identify a hit, an association of variables that produces a crystal. In some instances this will produce crystals with the desired characteristics. More often than not, a series of successive experiments, termed optimization, will need to be carried out in order to produce

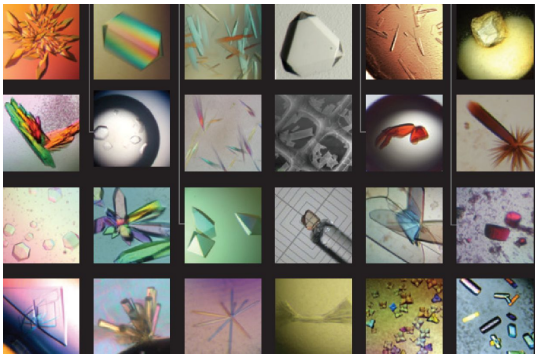

# CZYNNIKI CHEMICZNE I FIZYCZNE WPŁYWAJĄCE NA KRYSTALIZACJĘ BIAŁEK

**The Sample**

The sample is the most important variable in the crystallization experiment. Prepare, purify, handle, and store the sample with only the greatest care and respect. Manipulate the sample and refine its environment (buffer, reagent) as needed to produce the desired crystals.

**Homogeneity**

Purify, purify, then purify some more. Start with a pure, uniform population of the sample.

**Solubility**

Solubilize the sample in a sample buffer that is optimized with regard to pH, buffer, and excipients that dissolve the sample to high concentration free of aggregates, precipitate, or other phases. Pursue monodispersity not polydispersity.

**Stability**

Prepare and maintain the sample in a chemical and physical solution that promotes optimal stability of the sample. Do not allow the sample to go to the dark side, form oligomers, undergo significant conformational change, denature or change in any way before and during crystallization. Pursue a stable and unchanging sample.

**Supersaturation**

Find and pursue ways to move the sample into a supersaturated state. Using reagents, pH, temperature, and other variables to move sample equilibrium from a solution to a solid.

**Association**

Promote the orderly association of the sample molecules while avoiding non-specific aggregation, precipitate, or phase separation. Manipulate the chemical and physical environment to facilitate positive molecular interactions.

**Nucleation**

Promote and induce a few nuclei in a controlled manner. The number, size, and quality of the crystal depend upon the first nuclei and the mechanism of their growth. Manipulate the chemical and physical environment to produce limited nucleation and controlled growth.

| | |
|---|---|
| Purity of the sample | Genetic modifications |
| Conformational flexibility of the sample | Symmetry of the molecule |
| Homogeneity of the sample | Stability and level of denaturation of the sample |
| pH and buffer | Isoelectric point |
| Type and concentration of the precipitant (reagent) | His tags and other purification tags – presence or absence |
| Concentration of the sample | Thermal stability |
| Purity of the sample | pH stability |
| Additives, co-factors, ligands, inhibitors, effectors, and excipients | History of the sample |
| Chaotropes | Proteolysis |
| Detergents | Microbial contamination |
| Metals | Storage of the sample |
| Ionic strength | Handling of the sample and associate cleanliness |
| Reducing or oxidizing agents | Anion and cation type and concentration |
| Source of the sample | Degree of relative supersaturation |
| Presence of amorphous or particulate material | Initial and final concentration of the reagent |
| Post-translational modifications | Path and rate of equilibration |
| Chemical modifications | |


# CZYNNIKI CHEMICZNE I FIZYCZNE WPŁYWAJĄCE NA KRYSTALIZACJĘ BIAŁEK


**Nucleation**

Promote and induce a few nuclei in a controlled manner. The number, size, and quality of the crystal depend upon the first nuclei and the mechanism of their growth. Manipulate the chemical and physical environment to produce limited nucleation and controlled growth.

**Variety**

Pursue everything. Explore as many chemical, biochemical, and physical options and opportunities as possible for the growth and optimization of the crystal. Be thorough and relentless.

**Control**

Maintain control of the experimental system, at an optimal state, free of unknowns, perturbations, and fluctuations, from start to finish.

**Impurities**

Keep it clean. Avoid and discourage the presence, inclusion, and formation of impurities in the sample, reagent, and containers. This can minimize the incorporation of impurities into the crystal lattice, as well as minimize problems with reproducing experimental results.

**Preservation**

Take care of the crystal, protect them from shock, as well as chemical, biochemical, and physical change or disruption.


| | |
|---|---|
| Purity of the sample | Genetic modifications |
| Conformational flexibility of the sample | Symmetry of the molecule |
| Homogeneity of the sample | Stability and level of denaturation of the sample |
| pH and buffer | Isoelectric point |
| Type and concentration of the precipitant (reagent) | His tags and other purification tags – presence or absence |
| Concentration of the sample | Thermal stability |
| Purity of the sample | pH stability |
| Additives, co-factors, ligands, inhibitors, effectors, and excipients | History of the sample |
| Chaotropes | Proteolysis |
| Detergents | Microbial contamination |
| Metals | Storage of the sample |
| Ionic strength | Handling of the sample and associate cleanliness |
| Reducing or oxidizing agents | Anion and cation type and concentration |
| Source of the sample | Degree of relative supersaturation |
| Presence of amorphous or particulate material | Initial and final concentration of the reagent |
| Post-translational modifications | Path and rate of equilibration |
| Chemical modifications | |

Czynniki fizyczne wpływające na krystalizację

| | |
|---|---|
| Temperature | Electric and magnetic fields |
| Rate of equilibration | Surface of the crystallization device |
| Method of crystallization | Viscosity of the reagent |
| Gravity, convection, and sedimentation | Heterogeneous and epitaxial nucleants |
| Vibration and sound | Geometry of crystallization device |
| Volume of the sample and reagent | Time |
| Pressure | Dielectric property of the reagent |

| | |
|---|---|
| Vapor Diffusion (Sitting, Hanging, Sandwich) | Sequential Extraction |
| Batch (Microbatch with or without oil) | pH Induced |
| Dialysis (Microdialysis) | Temperature Induced |
| Free interface diffusion (Counter diffusion, liquid bridge) | Effector Addition (Silver Bullet) |
| Controlled Evaporation | |

Metody krystalizacji

## THE SAMPLE

The sample is the single most important variable in the crystallization experiment. Begin with a pure, homogeneous, stable, active sample. The sample should be as pure as possible, 95 to 98%, assayed by Coomassie stained SDS-PAGE. A homogeneous, active sample, free of contaminants, aggregates, and minimal conformational flexibility is desired.

Dynamic Light Scattering (DLS) can be used as a diagnostic for sample homogeneity, measuring the polydispersity of the sample, pointing out aggregation, which can be a deterrent to crystallization. DLS can be also used to screen and identify sample buffer components such as buffer, pH, ionic strength, excipients, additives, and other chemical variables, as well as temperature, towards optimization of the sample buffer formulation to maximize sample homogeneity.

# DSF

Differential Scanning Fluorimetry (DSF or Thermofluor®) can be used as a diagnostic for sample stability, measuring the temperature stability of the sample in the presence of chemical variables such as pH, buffer, ionic strength, excipients, and additives.

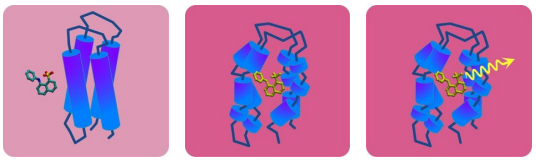

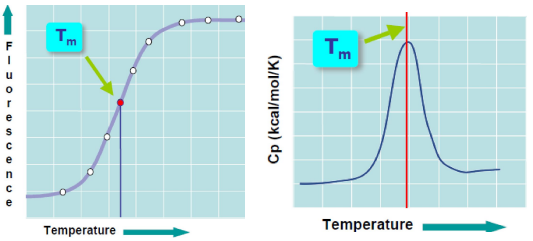


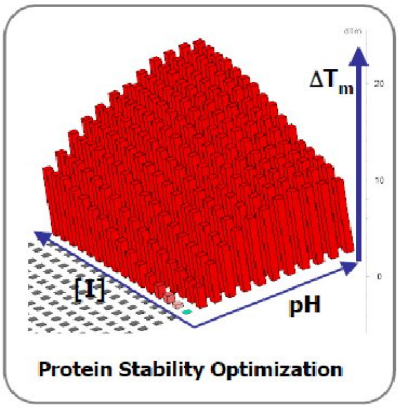


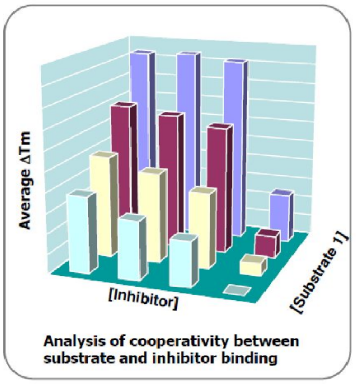


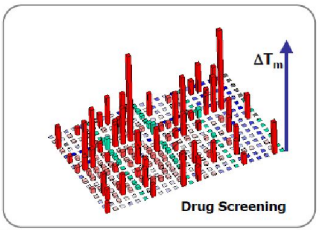

## HOMOGENEITY NOT HETEROGENEITY

Absolute homogeneity is essential for optimal crystallization as well as crystallographic analysis. An awareness of possible heterogeneity combined with methods and efforts to avoid and remove heterogeneity in the sample preparation should be a priority. Possible sources of sample heterogeneity include the following.

- Presence, absence, or variation in a bound prosthetic group, ligand, cofactor, or metal ion
- Variation in composition of carbohydrate on a glycoprotein
- Unintentional proteolytic modification
- Oxidation of sulfhydryl groups
- Reaction with heavy metals
- Presence, absence, or variation in post-translational side chain modification (methylation, amidation, phosphorylation, glycosylation, or lipidation)
- Variation in amino of carboxy terminus, or modification of the terminus
- Variation in aggregation or oligomer state
- Conformational flexibility or instability due to the dynamic nature of the sample
- Incomplete or incorrect refolding or partial denaturation
- Combining different preps or purifications

There are plenty of advantages to cloning, expressing and purifying the protein yourself, including the knowledge, control, and documentation of the experimental variables. One can also learn a great deal about the sample's behavior, solubility, and stability doing the work. However, it is often the case where someone else does the work leading up to and including the purification, and one might be handed the sample for crystallization. Either way, it is a good idea to characterize the protein before crystallization screening. Some variables to consider if you're handed a sample for crystallization include the following.

- What is the sample buffer?
- Was phosphate used at any time during the prep and purification?
- Are there disulfides or free cysteines?
- What ligands, substrates, co-factors, inhibitors, or metals are present or needed
- Are protease inhibitors present, is the sample sensitive to proteolysis?
- Has the protein or a similar protein previously been crystallized?
- At what pH range is the sample stable and unstable?
- At what temperature range is the sample stable or unstable?
- Is the protein glycosylated, methylated, phosphorylated?
- Are detergents present and if yes, what concentration?
- Is the sample a complex, dimer, trimer or ...?

## EXPERIMENT

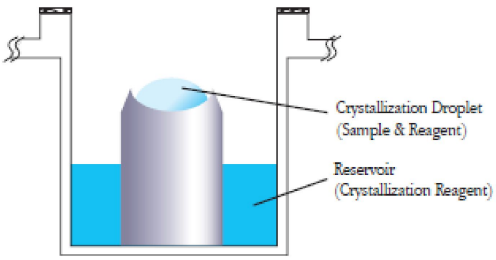


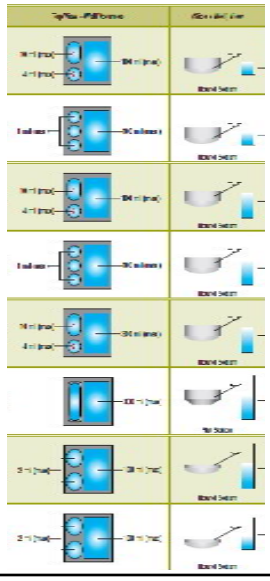

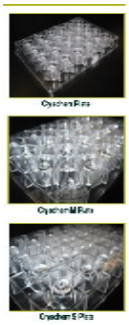

## HANGING DROP

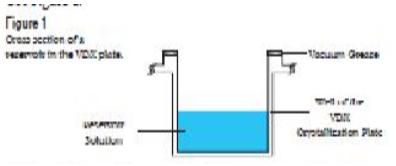


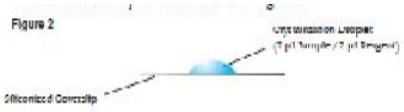


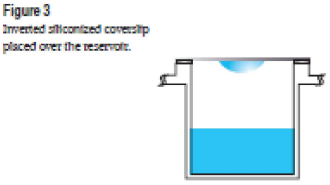


## MICROBATCH

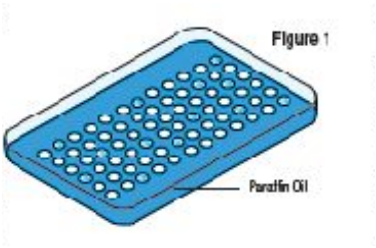


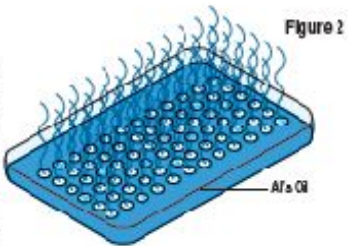

# DIALYSIS BUTTONS

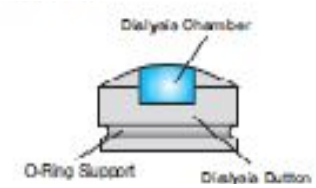


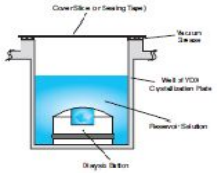

# SCREENING

Crystallization Screening

Crystallization screening is the process of evaluating methods, reagents, and other chemical and physical variables with the objective of producing crystals and/or identifying the variables which are positively or negatively associated with crystallization of the sample.

At the time of this writing, up to 40% of samples screened for crystallization will produce a crystal suitable for X-ray diffraction analysis. About 75% of proteins screened require optimization.

Optimization is the systematic manipulation and evaluation of variables which influence the crystallization of the sample.

Primary Screen

Primary screens are front line screens used for initial screening. If one does not have the knowledge or desire for a specific bias or focus on a reagent class, one may choose a sparse matrix screen composed of salts, polymer, organics, buffers at various pH levels, and mixtures thereof. Or one may have knowledge that a specific reagent class or mixture is desired and choose a screen biased for salt, polymer, polymer and salt, or other formulations.

Secondary Screen

Secondary screens are follow up screens to primary screens. The score from a primary screen such as Index may indicate crystals or promising results in polymer and polymer – salt mixtures. In such an instance, one may choose a secondary screen such as PEGRx 1 and PEGRx 2, as well as PEG/Ion and PEG/Ion 2. Or, primary screens may show promising scores in salt based reagents, where secondary screens such as SaltRx 1 and SaltRx 2 would be appropriate for follow up screening.

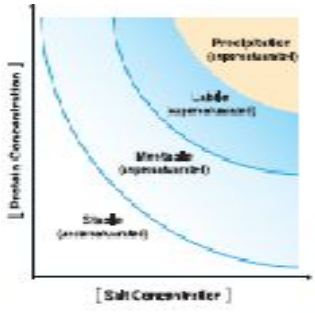

# SCREENING

Grid Screen

Grid Screens are simple, logical methods for systematically screening on a pH versus precipitant (reagent) grid. For example, the pH range 4 to 9 might be screened in 1 pH increments across the 6 wells of the X-axis of a 24 well crystallization plate, while a reagent, such as Polyethylene glycol 6,000 might be screened in 4 concentrations (5, 10, 20, 30% w/v) across the 4 wells of the Y-axis of a 24 well crystallization plate. The method depends on the ability to identify preliminary crystallization conditions while coarsely or finely sampling two variables, typically pH and reagent concentration. Grid Screening can be used as a primary or secondary screen strategy and is most often employed in optimization of initial crystallization conditions (hits). Grid Screens can be designed to cover a broad range of pH and reagent concentration in big steps, casting a broad net to identify an initial promising pH and reagent concentration (hit). Subsequently, successively finer grids can be generated to identify the optimal pH and reagent concentration for crystallization. The Grid Screen strategy was an original approach to protein crystallization, prior to the development and popularization of sparse matrix screening.

Sparse Matrix Screen

Sparse Matrix Screens are composed of a sampling of reagent formulations that have previously crystallized a protein. The formulations found in a Sparse Matrix Screen have emerged over time from the accumulated wisdom and experience of generations of many crystal growers. Initial ideas are assembled, formulated, and tested against previously crystallized and not yet crystallized proteins. Duds are dropped and winners move onto subsequent rounds of testing. Testing also employs formulations from the literature as well as databases, such as the Protein Data Bank (PDB)3, Biological Macromolecule Crystallization Database (BMCD)4-6, in house data, or data shared through centers and collaborators. When data mining, one must carefully review the data, as screens have existed long enough now that they themselves are within the database, and one must avoid getting caught in some local minima; one should also avoid cherry picking formulations to create a screen that, while looking good on paper, produces redundant hits, rather than sample an appropriate and balanced chemical space of home run conditions as

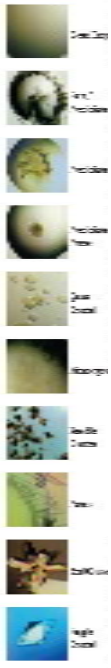

# CRYSTALLISATION

**Crystallization.** Purified GLP-1R StaR was crystallized using the vapour diffusion

method at 10 °C. A 0.1 μ l sample of the concentrated protein (approximately

3.0 mg ml−1) was mixed with 0.1 μ l of mother liquor in MRC 2-drop 96-well plates (Molecular Dimensions) using a Mosquito from TTP Labtech. 70–150 μ m rod-like crystals of GLP-1R StaR were grown in 100 mM Tris-HCl pH 8.0–9.0, 32–44% (v/v) polyethylene glycol 200.

Typically, crystals grew within 4 h but took 3–4 days to reach their maximum size.

Single crystals were cryo-protected in 0.1 M Tris-HCl pH 8.4, 40% PEG200, 12.5 mM HEPES pH 7.5, 75 mM NaCl, 0.005% POPG, 0.3% OTG and 0.1 μ M peptide 5, mounted using nylon cryo loops (Hampton Research), flash-frozen and then stored in liquid nitrogen until data collection.

https://www.youtube.com/watch?v=_iP-PclaY38

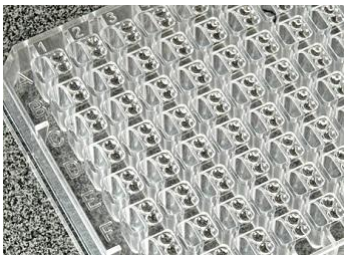

The fourth generation MRC Plate 96 well 2 Drop UV Crystallization Plate was designed by crystallographers at the MRC Laboratory of Molecular Biology in Cambridge, UK.

## MRC-2

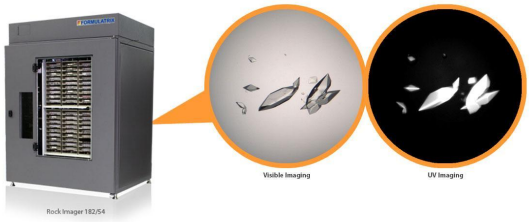


Features:

- Optically superior UV transmissible polymer
- Raised, wide wells make crystal retrieval easy.
- Conical wells for exceptional drop placement and viewing.
- Screening and crystallogenesis experiments can be performed in one plate (10 nL-5 µL drops).
- The reservoirs hold volumes from 50-100 µL.
- Navigate under a microscope easily with micronumbered wells.
- Top of the plate has wide surfaces for better sealing with tape.

## CRYOLOOPS

Hampton Research CryoLoops:

18 mm Mounted CryoLoops with 20 micron diameter nylon. Nylon loops are staked to hollow, stainless steel MicroTubes™ that are used to mount, freeze, and secure the crystal during cryocrystallographic procedures and X-ray data collection. The MicroTube on the 18 mm Mounted CryoLoops is 18 mm in length and ready to insert into CrystalCap Magnetic and CrystalCap HT. The 20 micron diameter nylon loops show minimal diffraction, are thin for fast cryo cooling of the crystal, strong, and aerodynamic.

https://www.youtube.com/watch?v=i2G1fYtjXt8

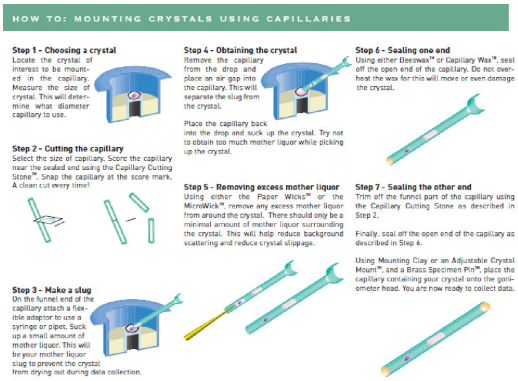


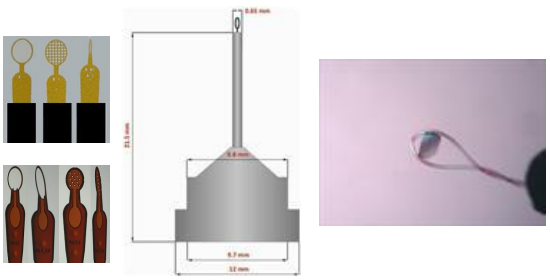

# ‚MIKROSKOP' DLA BIAŁEK

Mikroskop (stgr. μικρός mikros – "mały" i σκοπέω skopeo – „patrzę, obserwuję") – urządzenie służące do obserwacji małych obiektów, zwykle niewidocznych gołym okiem, albo przyjrzenia się subtelnym detalom obiektów małych, aczkolwiek widocznych nieuzbrojonym okiem.

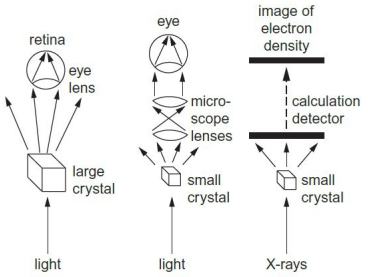


**Fig. 1.3** Left and centre, the function of the eye and microscope lenses for the recombination of scattered light; right, the equivalent two-stage process in X-ray diffraction.

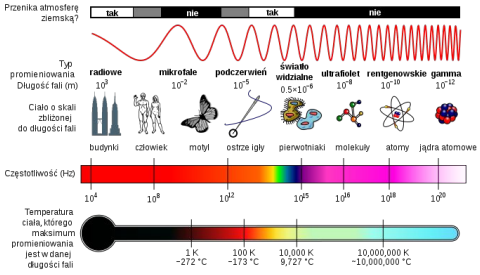


# MECHANIZM

**Refraction** is the alteration in the direction of travel of light as it passes from one medium into another with a different **refractive index**. It is responsible, for example, for the apparent bending of a drinking straw in a glass of water (and many other optical illusions), because water and air have quite different refractive indices. Refraction should not be confused with diffraction, a quite different phenomenon despite the similar name; even senior chemistry researchers sometimes produce nonsense words such as 'defraction'.

The **angstrom unit**, Å, is not strictly permitted by the SI rules, but is widely used in structural chemistry because of its convenient size: 1Å = 100 pm = 0.1nm.

Focusing of extremely high intensity X-rays can be achieved using special methods, but they are not of general application.

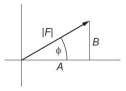


**Fig. 1.4** **Amplitude** and **phase** of a wave; the phase becomes important only when two or more waves meet and combine.

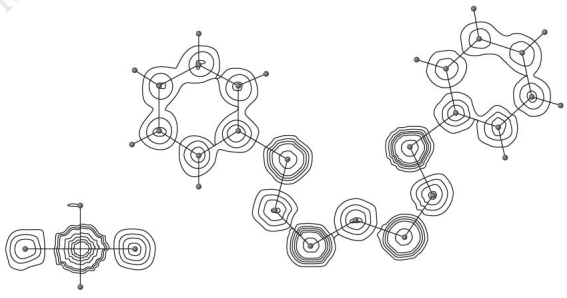

**Fig. 1.5** An electron density map, with the positions of atoms and bonds marked. Note that the rather wiggly contours here and in other figures are an artefact of the computer program used.

## KRYSZTAŁ

Ciało stałe, w którym cząsteczki (kryształy molekularne), atomy (kryształy kowalencyjne) lub jony (kryształy jonowe) są ułożone w uporządkowany schemat powtarzający się we wszystkich trzech wymiarach przestrzennych.

W objętości ciała cząsteczki zajmują ściśle określone miejsca, zwane węzłami sieci krystalicznej, i mogą jedynie drgać wokół tych położeń.

Każdy kryształ zbudowany jest z wielu powtarzających się komórek elementarnych. W zależności od ich rodzaju kryształy tworzą różne układy krystalograficzne.

Rodzaje ciał krystalicznych:

**monokryształy**, zwane krócej „kryształem" – uporządkowanie obejmuje całe ciało

**polikryształy** – uporządkowanie obejmuje fragmenty ciała.

## ELEMENTY SYMETRII

Zwykłe osie symetrii.

oś symetrii – prosta, wokół której powtarzają się jednakowe części kryształu, przy czym te części mogą się powtarzać co kąt α = 60°, 90°, 120°, 180°, 360°, liczbę n = 360°/α nazywa się krotnością osi symetrii; w kryształach możliwe są osie jedno-, dwu-, trzy- cztero-, sześciokrotne.

Płaszczyzna symetrii.

płaszczyzny symetrii – płaszczyzny dzielące kryształ na dwie części pozostające względem siebie w takim stosunku jak przedmiot do swego obrazu w zwierciadle płaskim.

Centrum symetrii (inwersji)

środek symetrii – punkt położony wewnątrz kryształu, który ma tę własność, że na dowolnej prostej przeprowadzonej przez ten punkt, w jednakowej od

Złożone elementy symetrii:

**oś inwersyjna** – działa w ten sposób, że dana część kryształu powtarza się dopiero po wykonaniu przekształceń względem środka i osi symetrii.

**oś przemienna (oś zwierciadlana)** – oś otrzymana przez sprzężenie osi symetrii z prostopadłą do niej płaszczyzną symetrii.

## KRYSZTAŁ – KOMÓRKA ELEMENTARNA

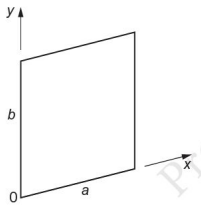


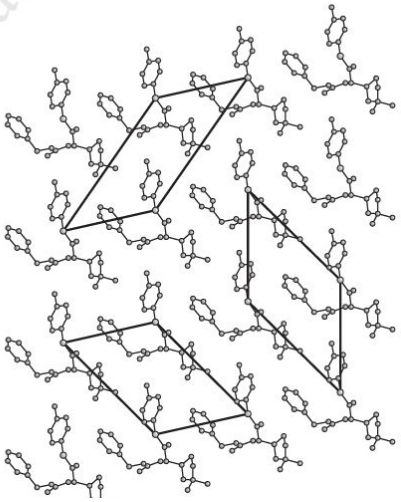

## KRYSZTAŁ – UKŁADY KRYSTALOGRAFICZNE

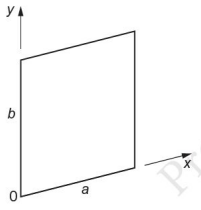


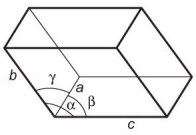


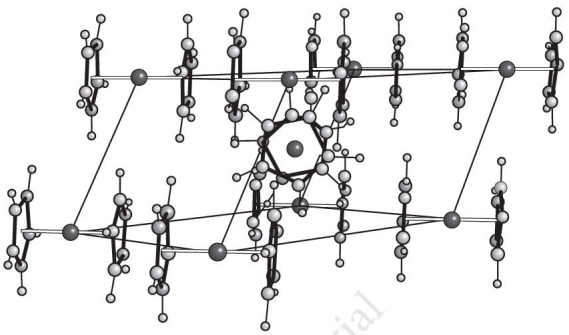

## KRYSZTAŁ – GRUPY PUNKTOWE (KLASY KRYSTALOGRAFICZNE)

Komórka elementarna - w krystalografii - najmniejsza, powtarzalna część struktury kryształu, zawierająca wszystkie rodzaje cząsteczek, jonów i atomów, które tworzą określoną sieć krystaliczną. Komórka elementarna powtarza się we wszystkich trzech osiach, tworząc zamknięta sieć przestrzenną, której główną cechą jest symetria. Komórka elementarna ma zawsze kształt równoległościanu.

Poprzez translacje komórki elementarnej o wektory będące całkowitymi wielokrotnościami wektorów sieci krystalicznej otrzymuje się całą sieć krystaliczną kryształu.

**Table 1.1** Crystal systems

| Crystal system | Essential symmetry | Restrictions on unit cell |
|---|---|---|
| Triclinic | none | none |
| Monoclinic | one twofold rotation and/ or mirror | $\alpha = \gamma = 90°$ |
| Orthorhombic | three twofold rotations and/ or mirrors | $\alpha = \beta = \gamma = 90°$ |
| Tetragonal | one fourfold rotation | $a = b$; $\alpha = \beta = \gamma = 90°$ |
| Trigonal | one threefold rotation | $a = b$; $\alpha = \beta = 90°$; $\gamma = 120°$ |
| Hexagonal | one sixfold rotation | $a = b$; $\alpha = \beta = 90°$; $\gamma = 120°$ |
| Cubic | four threefold rotation axes | $a = b = c$; $\alpha = \beta = \gamma = 90°$ |

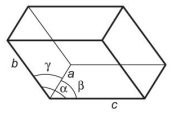


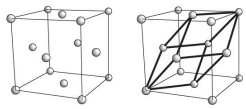

## GRUPY PRZESTRZENNE

Elementy symetrii niezbędne do wyznaczenia wszystkich punków równoważnych w krysztale opisane są dla wszystkich 230 grup w tomie A Międzynarodowych Tablic Krystallograficznych.

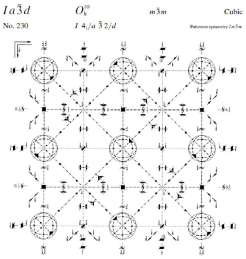


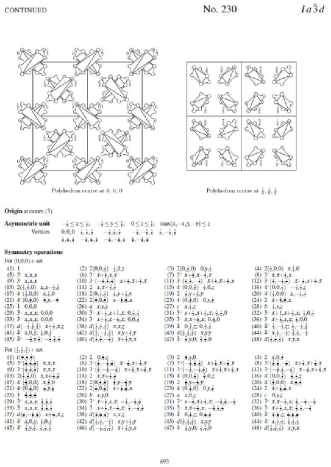

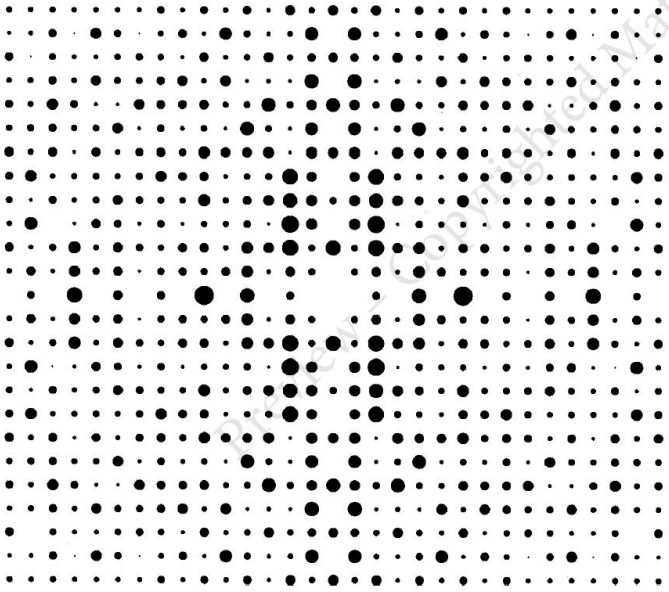

## DIFFRACTION DATA COLLECTION AND PROCESSING

Diffraction data collection and processing. X-ray diffraction data were measured on a Pilatus 6M detector at Diamond Light Source beamline I24 using a beam size of 10 μ m × 10 μ m.

Crystals displayed diffraction initially out to approximately 3.6 Å following exposure to a non-attenuated beam for 0.2 s per 0.2° of oscillation.

It was possible to collect about 12° of useful data from each crystal before radiation damage became too severe. Data from individual crystals were integrated using XDS. A complete dataset to 3.7 Å was obtained by merging diffraction data from eight crystals belonging to the trigonal space group P3121. Data merging and scaling were carried out using the program AIMLESS from the CCP4 suite of programs. Data collection statistics are recorded in

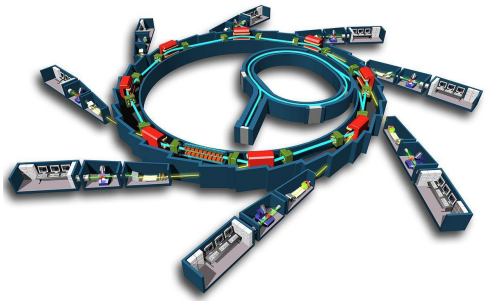

## SYNCHROTRON

Synchrotrony to akceleratory elektronów i źródła wyjątkowego, synchrotronowego światła. Akceleratory cząstek są urządzeniami badawczymi, które przyspieszają cząstki elementarne posiadające ładunek elektryczny do prędkości bliskiej prędkości światła. W synchrotronach w momencie, gdy tor lotu cząstek jest zakrzywiany, pojawia się strumień fotonów – światło synchrotronowe. Jasność tego światła jest miliardy razy większa od jasności światła słonecznego. Obejmuje ono szeroki zakres fal elektromagnetycznych: od podczerwieni do promieniowania rentgenowskiego. Fale te mogą być filtrowane i kierowane do wielu linii badawczych na potrzeby różnorakich analiz.

Synchrotrony pozwalają zajrzeć w głąb materii i dokonać jej precyzyjnych analiz. Dzięki nim naukowcy mogą badać zarówno skład badanej substancji, jak i jej strukturę – światło synchrotronu może przenikać do wnętrza badanej materii. Może odwzorowywać z dowolną szczegółowością ukryte warstwy lub ich wybrane fragmenty, bez uszkadzania tych położonych na zewnątrz. Promieniowanie synchrotronowe stymuluje również procesy zachodzące w materii – wywołuje zmiany w badanych obiektach.

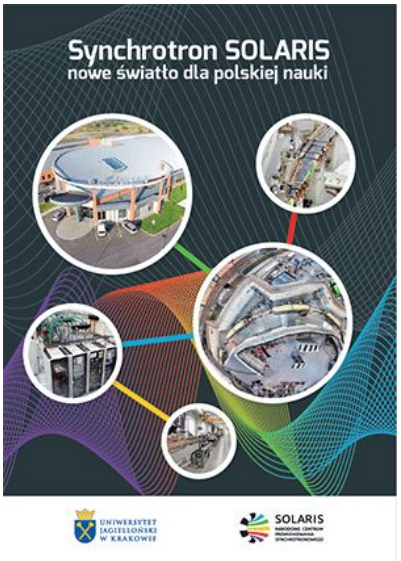


## LINIE BADAWCZE

W chwili obecnej w Centrum SOLARIS uruchamiane są dwie linie badawcze:

- linia PEEM/XAS.

LINIA PEEM/XAS (Photoemission Electron Microscopy / X-ray Absorption Spectroscopy) - linia wykorzystuje promieniowanie synchrotronowe emitowane przez magnes zakrzywiający i jest dedykowana do pomiarów mikroskopowych i spektroskopowych w zakresie miękkiego promieniowania rentgenowskiego. Powstaje w ramach współpracy SOLARIS z Instytutem Katalizy i Fizykochemii Powierzchni im. Jerzego Habera Polskiej Akademii Nauk oraz Akademią Górniczo-Hutniczą im. Stanisława Staszica w Krakowie.

Stacje końcowe:

**Stacja pomiarowa PEEM (Photoemission Electron Microscopy)** - mikroskop fotoelektronowy, wykorzystujący niskoenergetyczne elektrony wzbudzone fotonami do obrazowania powierzchni z przestrzenną zdolnością rozdzielczą kilkudziesięciu nanometrów.

**Stacja pomiarowa XAS (X-ray Absorption Spectroscopy)** uniwersalna stacja do badania widm absorpcji rentgenowskiej.

- linia UARPES.

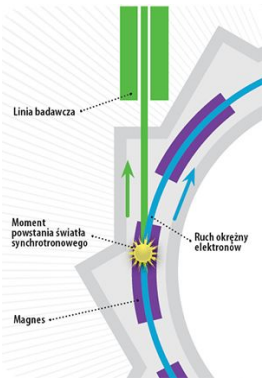


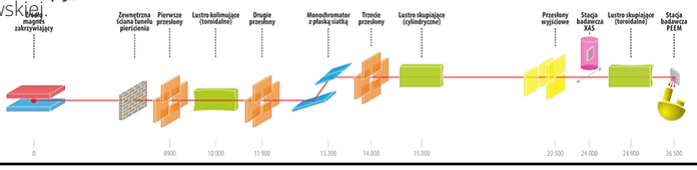

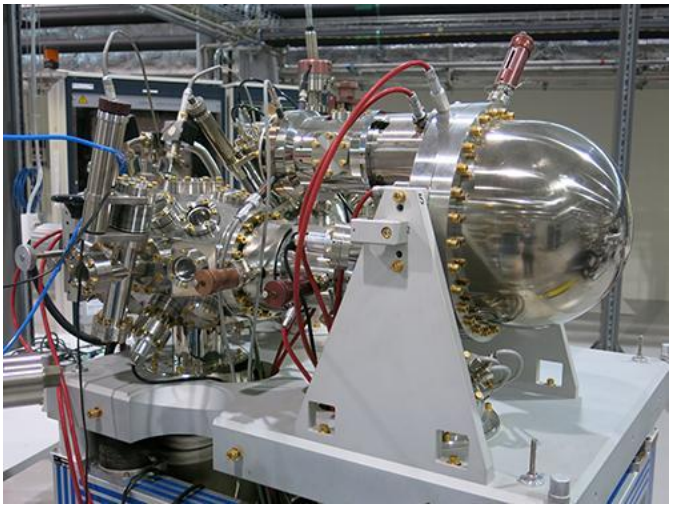

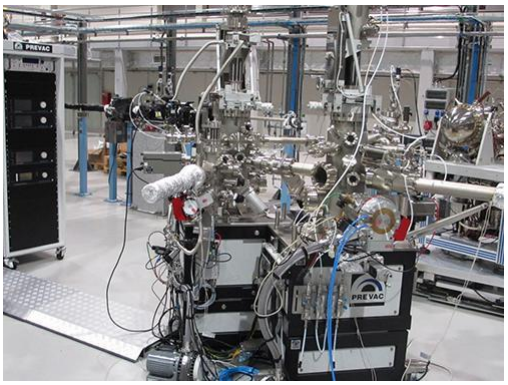

## DATA COLLECTION

Crystals displayed diffraction initially out to approximately 3.6 Å following exposure to a non-attenuated beam for 0.2 s per 0.2° of oscillation.

It was possible to collect about 12° of useful data from each crystal before radiation damage became too severe. Data from individual crystals were integrated using XDS. A complete dataset to 3.7 Å was obtained by merging diffraction data from eight crystals belonging to the trigonal space group P3121. Data merging and scaling were carried out using the program AIMLESS from the CCP4 suite of programs. Data collection statistics are reported in Extended Data Table 2.

https://youtu.be/XvkrgWKD6XI

# DATA PROCESSING

1: Determination of crystal orientation, cell parameters and spacegroup

Autoindexing Interactively
Autoindexing when running the program in background
REFIX and general notes
DPS Indexing in background
Autoindexing using different images from the same crystal

2: Running the STRATEGY and TESTGEN options

Overview of the STRATEGY option
Some Examples of the STRATEGY options
Determining the oscillation angle for each image (TESTGEN option)

3: Determining Accurate Cell parameters
Using Post-refinement to refine the cell

4: Collecting data and processing the images

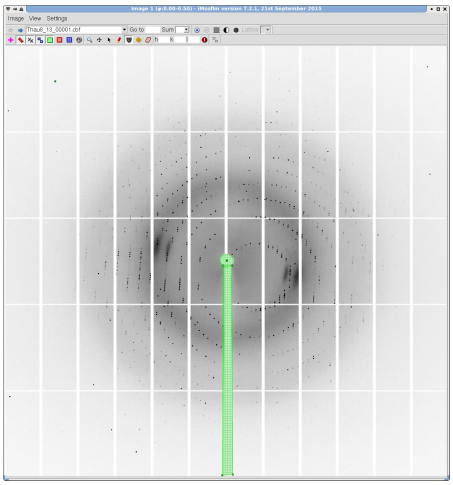

# DATA PROCESSING

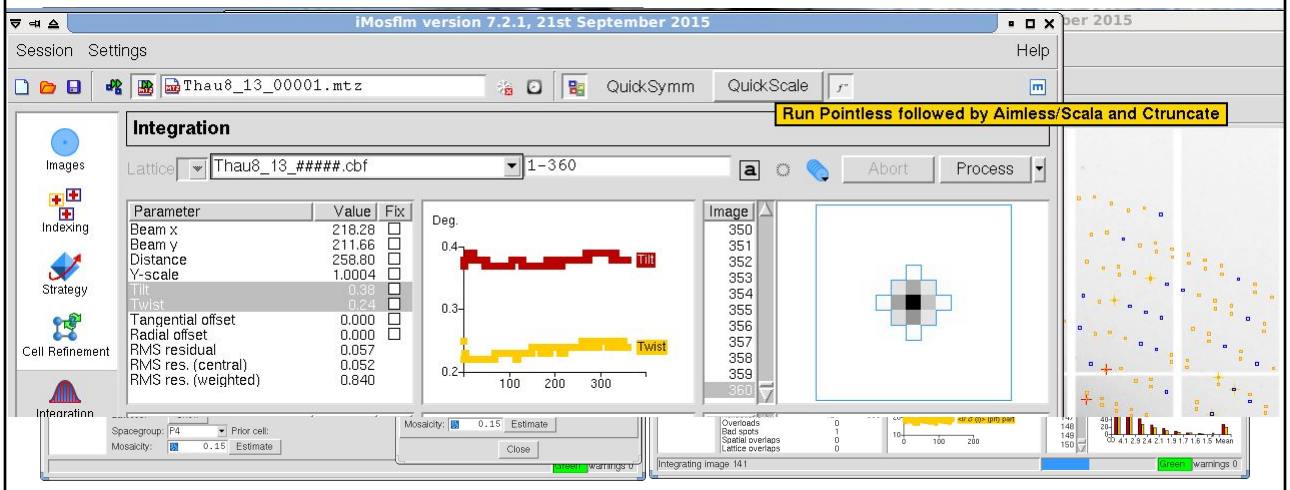

NMR

# Spektroskopia magnetycznego rezonansu jądrowego

- Spektroskopia NMR (skrótowiec z ang. nuclear magnetic resonance) – technika spektroskopowa obserwacji lokalnych pól magnetycznych wokół jąder atomowych.

- Próbkę umieszcza się w polu magnetycznym, a sygnał NMR wytwarza się przez wzbudzenie próbki za pomocą fal radiowych w magnetycznym rezonansie jądrowym, który jest wykrywany przy użyciu czułych odbiorników radiowych.

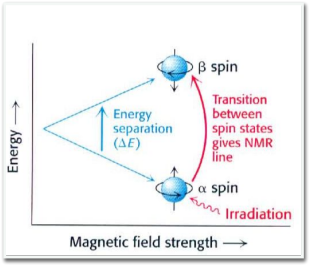

# Podstawy fizyczne

- Niezerowy spin jądrowy s mają praktycznie wszystkie atomy o nieparzystej liczbie nukleonów:
  - wodór 1H, węgiel 13C, azot 15N, tlen 17O, fluor 19F, sód 23Na i fosfor 31P).
- W bardzo dużym uproszczeniu spin jądrowy można sobie wyobrazić jako rotację jądra wokół własnej osi. Jest on związany z wewnętrznym momentem pędu jądra.

- Podstawą zjawiska NMR jest oddziaływanie spinów jądrowych z polami magnetycznymi:
  - stałym polem magnetycznym, które jest wytwarzane przez magnesy,
  - zmiennym polem magnetycznym skierowanym prostopadle do osi stałego pola magnetycznego (generowanym przez fale elektromagnetyczne w cewce spektrometru),
  - zmiennymi polami lokalnymi generowanymi przez sąsiednie jądra atomów oraz związane z nimi elektrony.

# Podstawy fizyczne

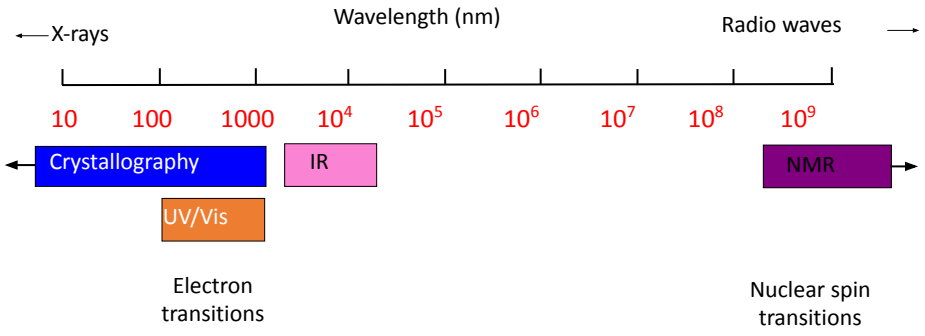

# Podstawy fizyczne

| Nucleus | I | # Protons | # Neutrons |
|---|---|---|---|
| $^{1}H$ | 1/2 | 1 | 0 |
| $^{12}C$ | 0 | 6 | 6 |
| $^{13}C$ | 1/2 | 6 | 7 |
| $^{14}N$ | 1 | 7 | 7 |
| $^{15}N$ | 1/2 | 7 | 8 |

Absorption of energy by nucleus - depends on nuclear spin

(I) = sum of **unpaired** protons + neutrons (spin 1/2)

# Wzbogacanie składu izotopowego

Skład izotopowy białek musi być wzbogacony w trakcie syntezy białek.

zastosowanie pożywek o zmodyfikowanym składzie izotopowym oraz odpowiednich szczepów ekspresyjnych.

znakowanie domen.

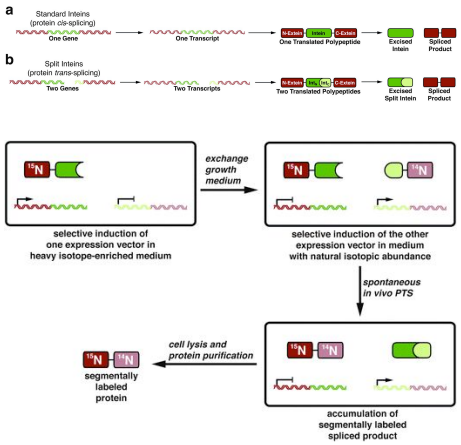

# Pomiar

Stężona próbka białka:

1 mM lub 15 mg/ml$^{-1}$ dla białka 15 kDa

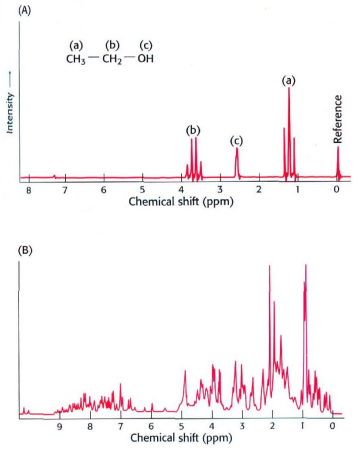


# Podstawy fizyczne

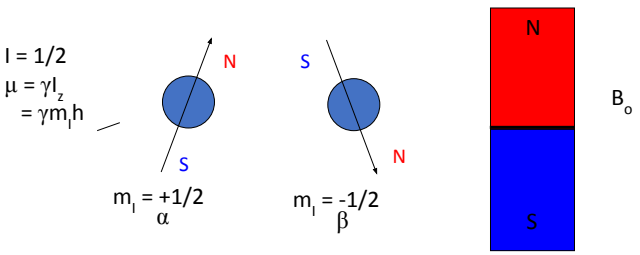


m=(-I, -I+1 ….I-1, I)

# Podstawy fizyczne

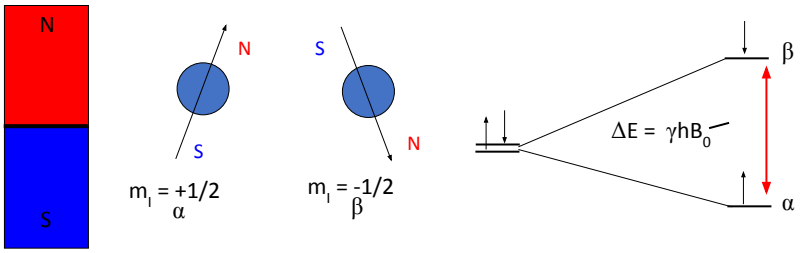


# Podstawy fizyczne

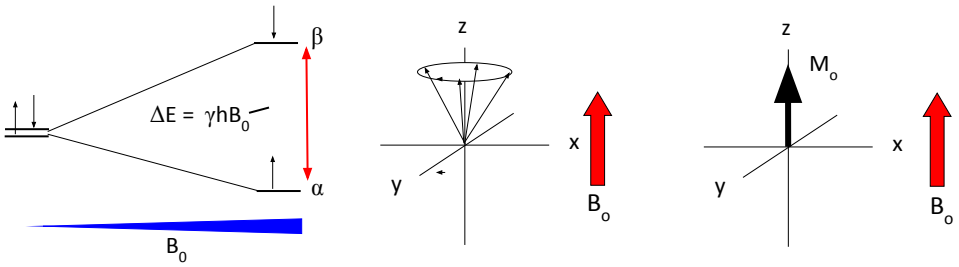


$B_0$ = 11.75 T (500 MHz)
14.09 T (600 MHz)
18.79 T (800 MHz)

As $B_0$ ↑ so does ΔE !

# Podstawy fizyczne

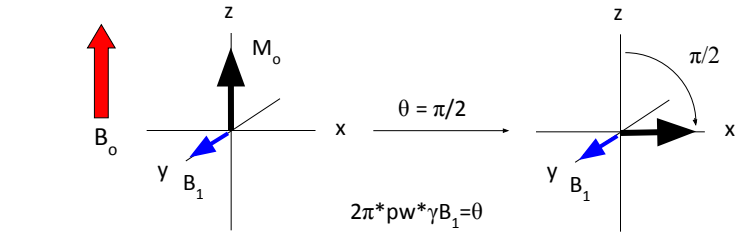


$2\pi * pw * \gamma B_1 = \theta$

$$pw = \frac{1}{4 * \gamma B_1}$$

pw = 6 µsec $\gamma B_1$ = 41 kHz


# Podstawy fizyczne

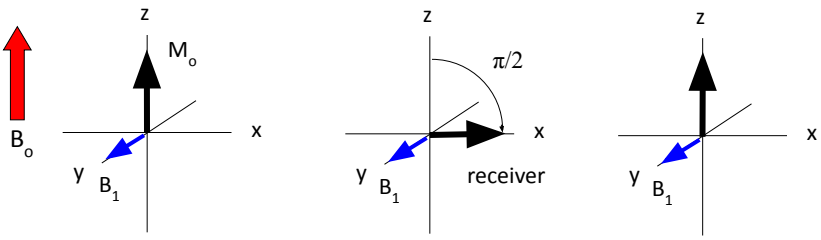


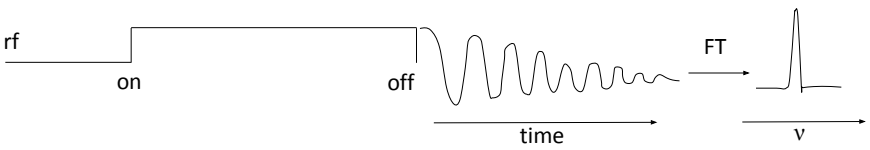

# Podstawy fizyczne

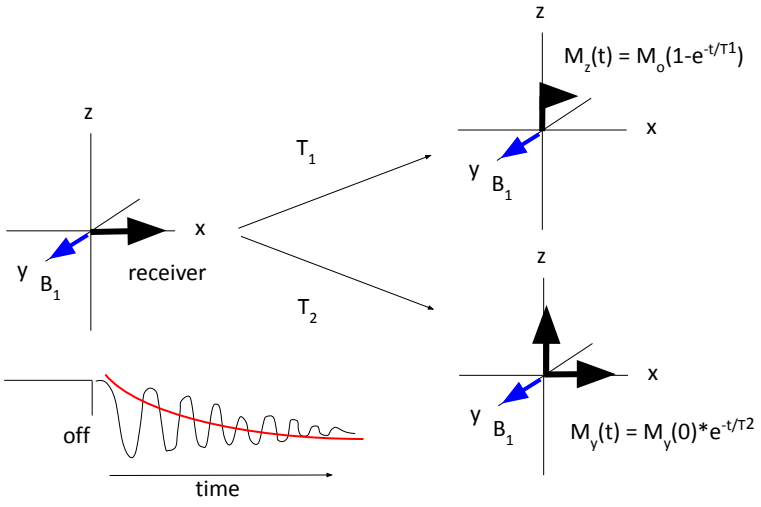


# Podstawy fizyczne

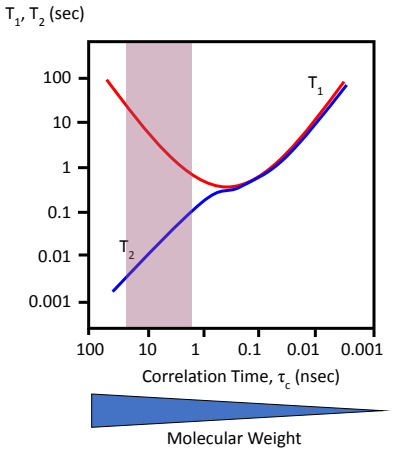


Linewidths

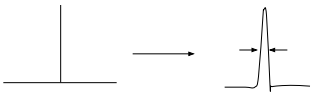

$\nu_{1/2} = \frac{1}{\pi T_2^*}$

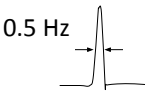

0.5 Hz

MW 100

10 Hz

MW 20,000

Principles of Protein NMR Spectroscopy

NMR Instrumentation

Magnet - $B_o$ 18.79 T


22.31 T (2006)

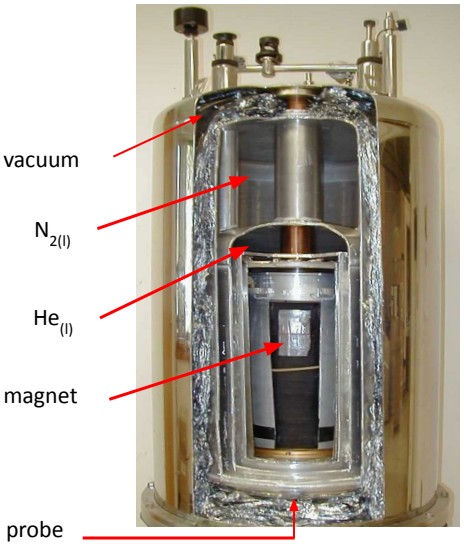


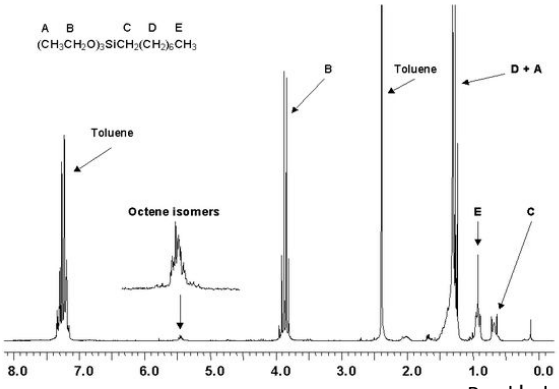


Przykład widma $^1$H NMR, wykonanego z użyciem aparatu Bruker DRX500, w CBMiM PAN, w cieczy (trietoksy-1-oktylosilan zanieczyszczony toluenem i izomerami oktenu)

# Analiza

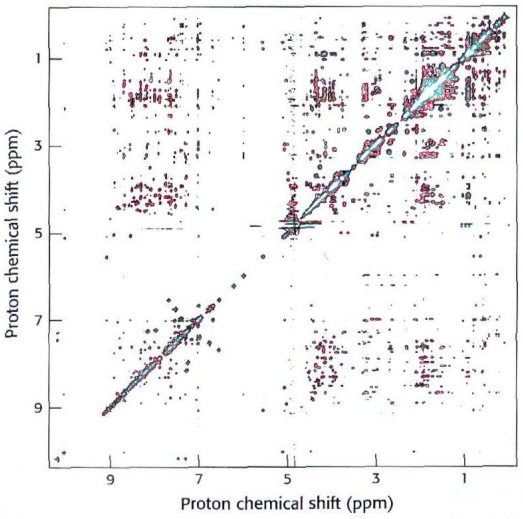


# Rodzaje widm

- Rodzaje widm NMR
- Widma n-wymiarowe w fazie ciekłej
  - analizowana próbka musi być ciekła (sama substancja może być ciekła lub stała, ale do analizy należy ją rozpuścić w rozpuszczalniku deuterowanym, tj. takim, w którym wszystkie lub możliwie wiele protonów zostało zastąpionych deuteronem).
  - analizowana substancja musi być rozpuszczona w rozpuszczalniku deuterowanym. Rejestruje się jednocześnie widma pochodzące od dwóch lub więcej rodzajów atomów, co umożliwia obserwację interferencji i sprzężeń między widmami generowanymi przez różne atomy w cząsteczce. Poza tym dosyć często stosuje się widma korelacyjne uwzględniające jądrowy efekt Overhausera co pozwala na określanie z dosyć dobrą skutecznością faktycznych odległości przestrzennych pomiędzy oddziaływających ze sobą w ten sposób jądrami. Widma tego typu są szczególnie przydatne w ustalaniu przestrzennej struktury cząsteczek o złożonej budowie.
- Widma w fazie stałej – analizowana substancja jest ciałem stałym – umożliwia ona np. obserwację sposobu uporządkowania kryształów. Ze względu na to, że w ciele stałym praktycznie każdy atom jest w nieco innym otoczeniu chemicznym jest to technika trudna, wymagająca m.in. stosowania „tricków” z wycinaniem szumu z widm.

# Historia

History

| | | |
|---|---|---|
| 1946 | Bloch, Purcell | first nuclear magnetic resonance |
| 1955 | Solomon | NOE (nuclear Overhauser effect) |
| 1966 | Ernst, Anderson | Fourier transform NMR |
| 1975 | Jeener, Ernst | 2D NMR |
| 1985 | Wüthrich | first solution structure of a small protein (BPTI) from NOE based distance restraints |
| | → NMR is about 25 years younger than X-ray crystallography | |
| 1987/8 | | 3D NMR + $^{13}C$, $^{15}N$ isotope labeling |
| 1996/7 | | new long range structural parameters: |
| | | - projection angles from: residual dipolar couplings (partial alignment) |
| | | $T_1/T_2$ relaxation time ratio (anisotropic diffusion) |
| | | - projection angles (cross-correlated relaxation) |
| | | - TROSY (molecular weight > 100 kD) |

Nobel prizes

| | | |
|---|---|---|
| 1944 | Physics | Rabi (Columbia) |
| 1952 | Physics | Bloch (Stanford), Purcell (Harvard) |
| 1991 | Chemistry | Ernst (ETH) |


Felix Bloch & Edward Purcell
Physics-1952

Richard Ernst
Chemistry -1991

Kurt Wuthrich
Chemistry-2002


Paul Lauterbur & Peter Mansfield
Medicine-2003

Brian Sykes

Lewis Kay

# Wykorzystanie NMR

- Wyznaczenie struktury 3d
- Określenie zmian dynamicznych struktury w skali picosek-sek
- Określenie stanów równowagowych
- Analiza procesu fałdowania

PDB entries 07-May-2002

| | Proteins | Protein/DNA Protein/RNA | DNA/ RNA | Carbo- hydrates |
|---|---|---|---|---|
| X-ray | 13580 | 649 | 610 | 14 |
| NMR | 2236 | 84 | 443 | 4 |

# Wady/zalety NMR

- Badania w fazie ciekłej
- Próbka nie ulega zniszczeniu
- Informacje uzyskujemy na poziomie pojedynczych aminokwasów

# Metodyka pomiaru

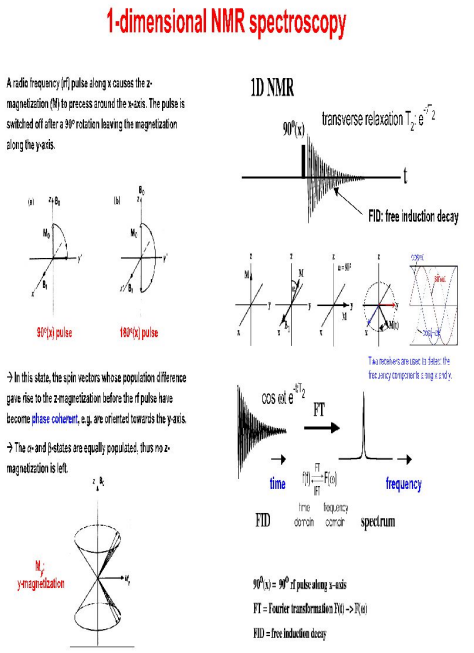

# Metodyka pomiaru

## Relaxation

After the rf pulse, the Boltzmann equilibrium is restored by relaxation. This is a result of interactions of the spins with each other and with the environment (the "lattice").

→ The equilibrium z-magnetization, $M_0$ is restored by longitudinal or spin-lattice relaxation which is described by a relaxation time constant $T_1$.

$$M_z(t) - M_0 = [M_z(0) - M_0] \exp(-t/T_1)$$

$T_1$ is measured by inverting the equilibrium z-magnetization $M_z(t) = -M_z$ and measuring the recreation of $+M_z$ magnetization in inversion recovery experiments ($180°$–$\tau$ – $90°$FID).

→ The decay of x,y magnetization reflects the loss of phase coherence of the spin vectors in the x,y plane and is called transverse or spin-spin relaxation described by a relaxation time constant $T_2$.

$$M_x(t) = M_x(0) \exp(-t/T_2)$$

$T_2$ is measured as the decay of transverse (x- or y-magnetization), for example using a spin-echo sequence ($90°$–$\tau$ – $180°$–$\tau$ FID) with a variable delay $\tau$.

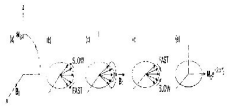

Hahn spin-echo experiment

$T_1$ and $T_2$ depend on the correlation time $\tau_c$ for random molecular tumbling (thus, on the molecular weight) and also on the B0 magnetic field strength:

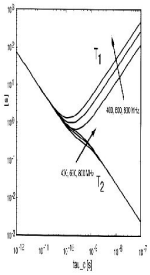


# Wpływ środowiska

## Chemical shifts

- At the local position of a nuclear spin within a molecule the external magnetic field $B_0$ is shielded by the local electronic environment. The external field is therefore scaled ($\sigma$ = shielding constant) : $B = B_0(1-\sigma)$.
- As a result, for example, the $H^N$ and $H_{C\alpha}$ protons in the peptide backbone of a protein have different chemical shift regions which helps to identify them.
- Chemical shifts are normalized with respect to the static magnetic field and expressed as ppm.

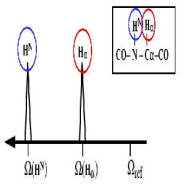


$$\delta(\text{ppm}) = (\Omega - \Omega_{ref})/\Omega_0 * 10^6$$

chemical shifts in parts per million [ppm] are *independent* of the field strenght of the static magnetic $B_0$ field

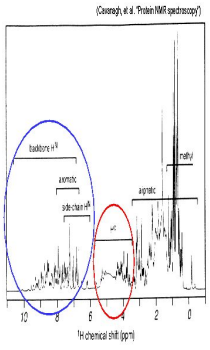

# Scalar/J-coupling

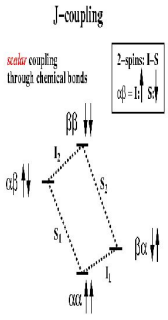


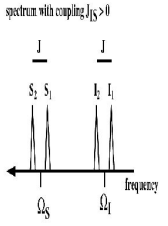


Sign of J-coupling

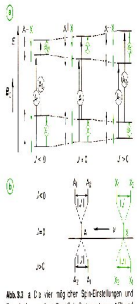

Multiplicities

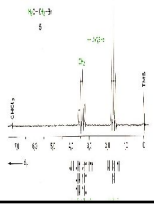

# 2D NMR: COSY

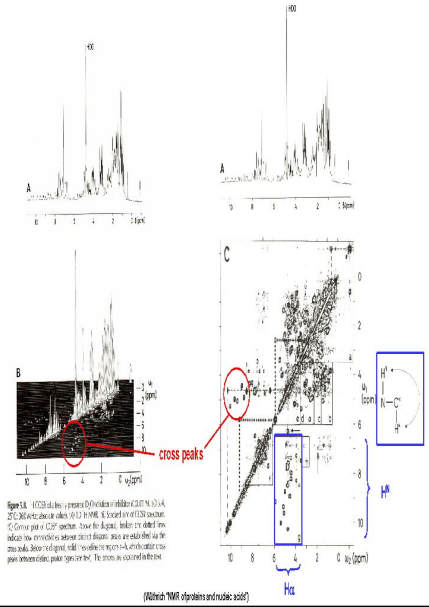


(Wüthrich 'NMR of proteins and nucleic acids')

## Heteronuclear 2D NMR: H,N correlations

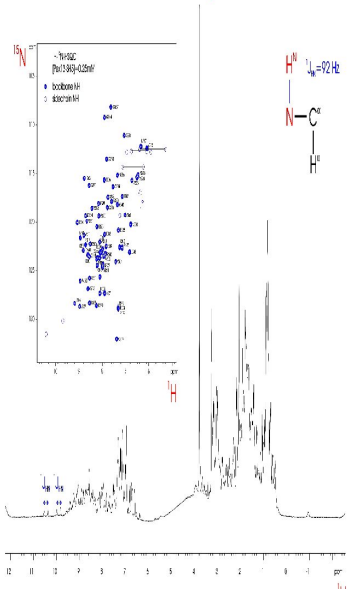


## Nuclear Overhauser Effect (NOE)

NOE

$$I \xrightarrow[\text{distance } r]{\text{dipolar coupling}} S$$

*dipolar* coupling through space
-> splitting (in solid phase)
-> relaxation (in liquid phase)

The NOE is a result of spin-spin cross relaxation via $W_2$ and $W_0$ transition rates between two spins I and S.
The NOE is inverse proportional to the distance between the two interacting spin.

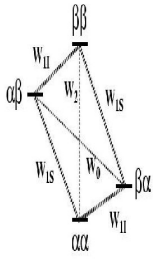


W = transition rates

NOE intensity ~ $1/r^6$

This distance dependence of the NOE is used to derive proton/proton distance restraints for the structure determination by NMR.

# Wyznaczanie struktury

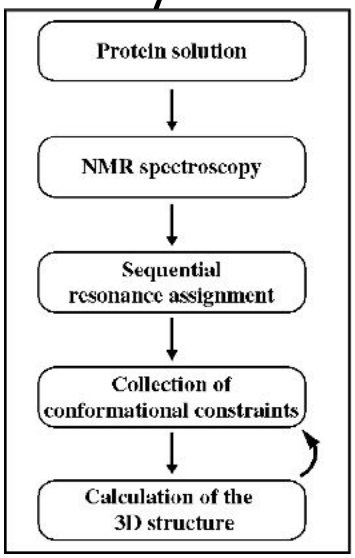


# Pomiar

Uproszczenie widma NMR osiąga się poprzez zastosowanie odpowiednich metod pomiarowych:

jądrowego efektu Overhausera (NOE) w technice spektroskopii jądrowego efektu Overhausera (NOESY);

spektroskopii korelacyjnej (COSY);

całkowitej spektroskopii korelacyjnej (TOCSY)

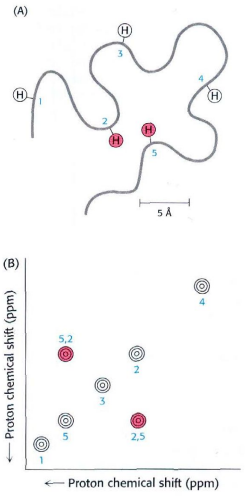

# Analiza

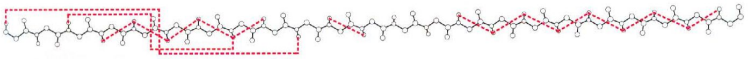

W trakcie interpretacji widm (ręcznej lub automatycznej) stosuje się następujące typy ograniczeń:

odległości;

kątów;

orientacji przestrzennej.

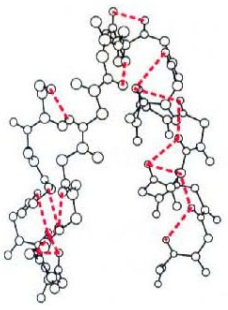

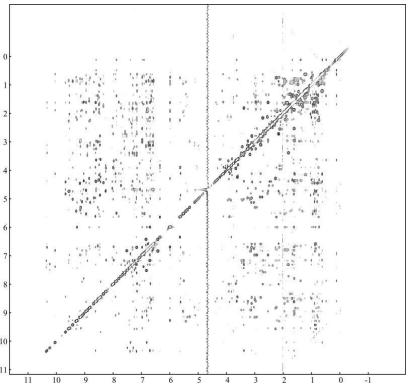

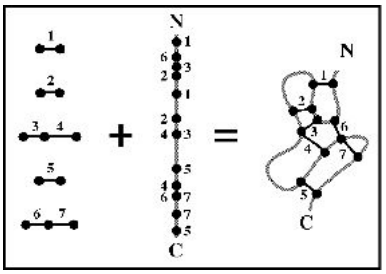


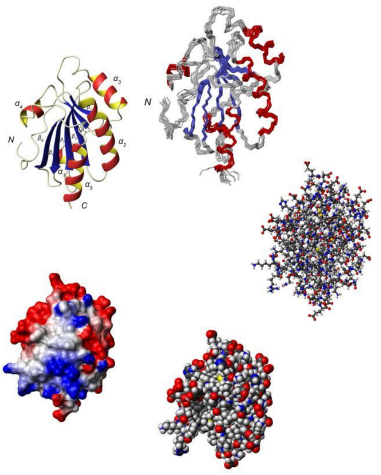

# Wynik

Wynikiem pomiarów jest rodzina struktur.

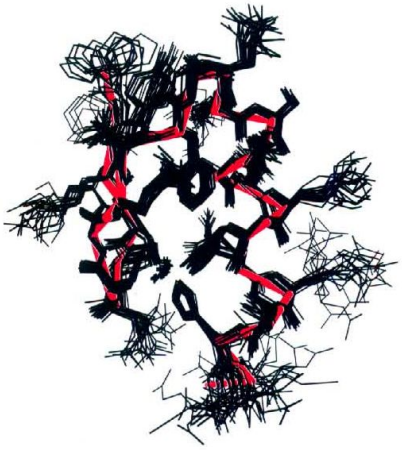

# Możliwe zastosowanie
Dynamika białek

- Procesy biologiczne nie są statyczne:
  - Przemiany strukturalne
  - Reakcje chemiczne enzymów
- Zrozumienie dynamiki procesów biologicznych pozwala na usprawnienie aspektów inżynierii białek

# Problem niskich stężeń w procesach biologicznych

- Procesy biologiczne:
  - Interakcje czwartorzędowe
  - Przenoszenie sygnałów
  - Kataliza enzymatyczna
  - Fałdowanie
  - Sygnalizacja allosteryczna

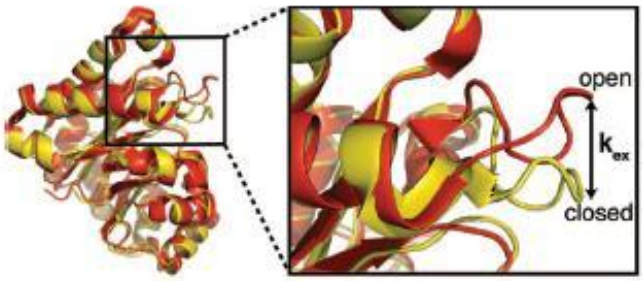

# Fałdowanie/kataliza enzymatyczna

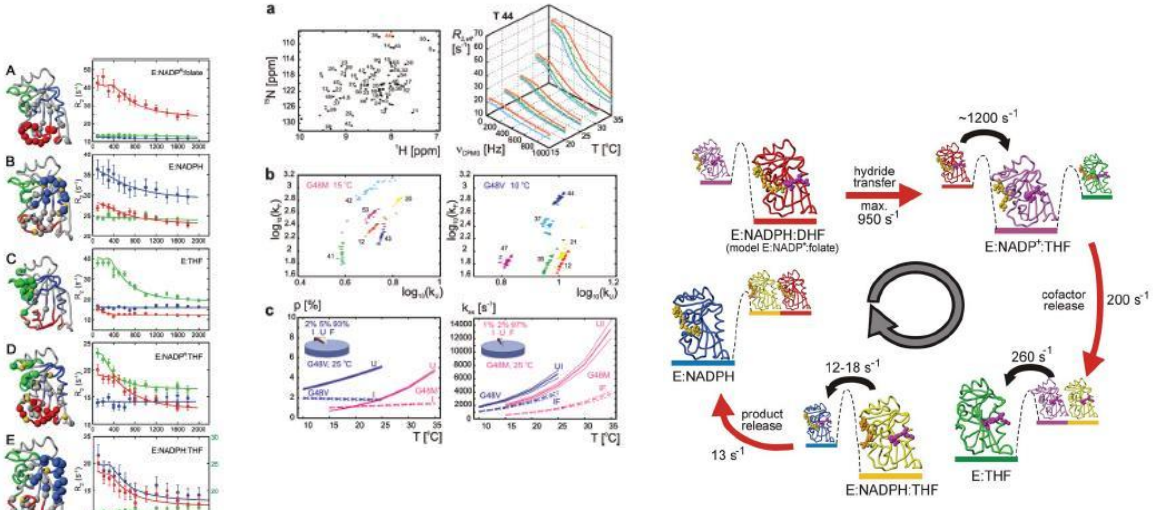


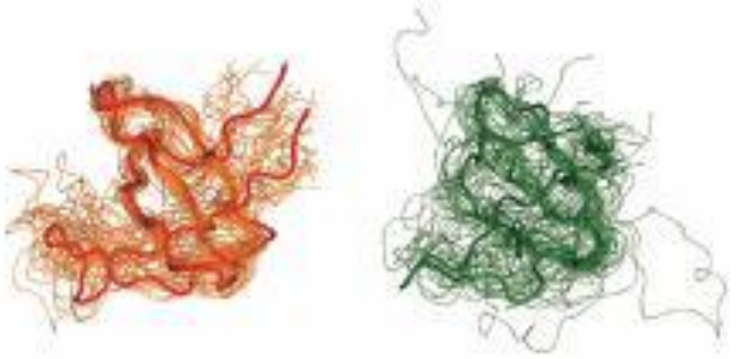

# Analiza konformacyja thioredoksyny

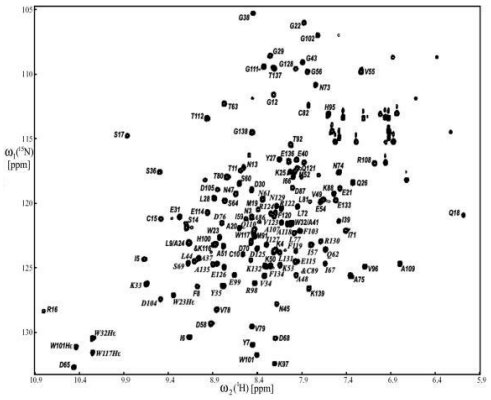

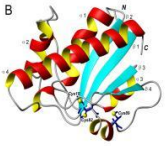

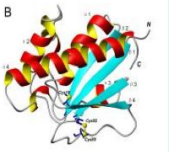

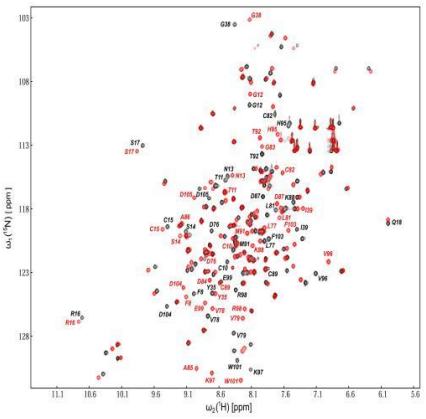

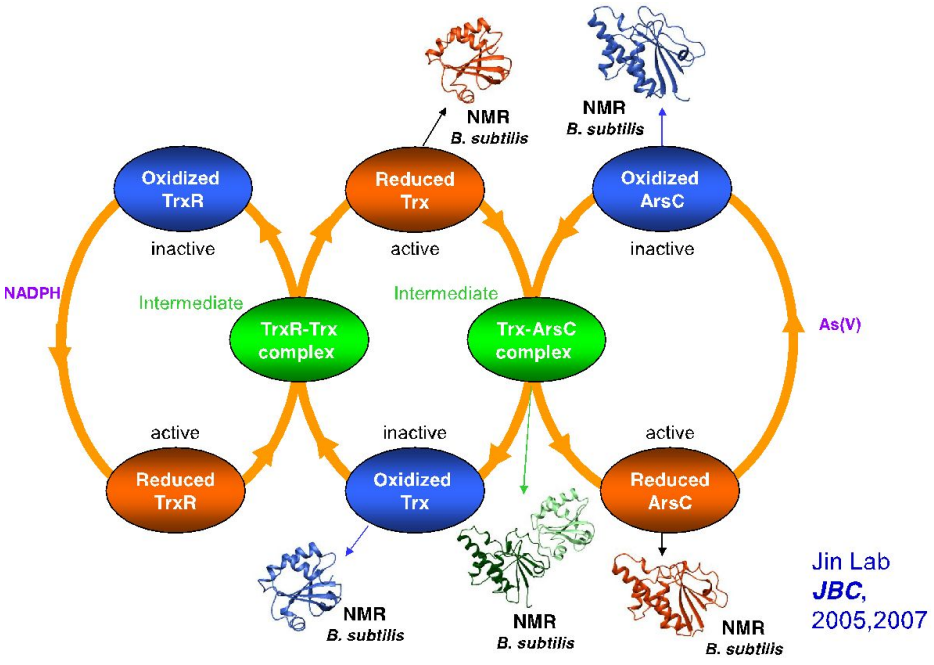


Jin Lab
***JBC***,
2005,2007

# Badanie oddziaływań

Metoda anazlizy perturbacji przesunięć chemicznych

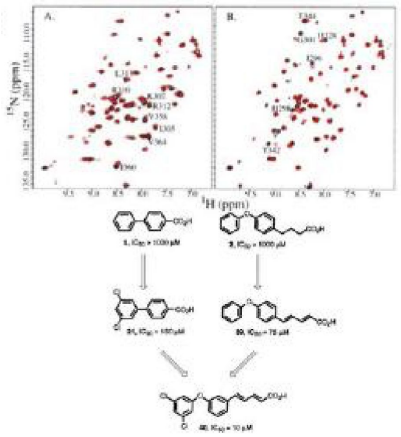

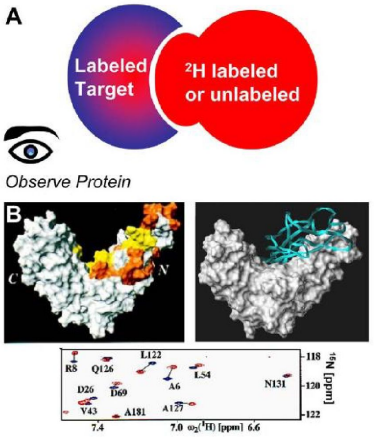


# Analiza białek błonowych

Problemy w analizie białek błonowych:

- Ekpresja
- Przygotowanie próbki
- Deuteracja i renaturacja

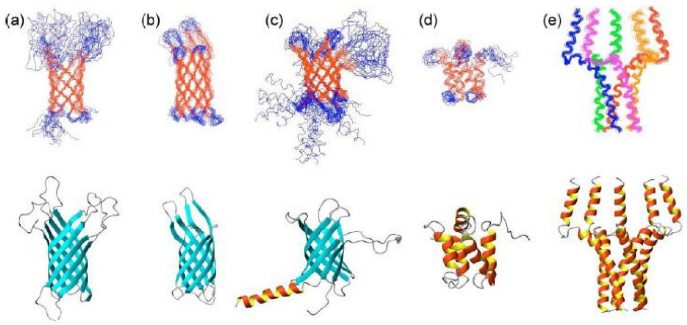

# Projektowanie i optymalizacja substancji aktywnych biologicznie
# SAR (structure activity reletionship)

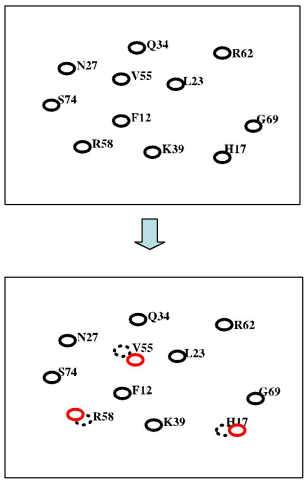


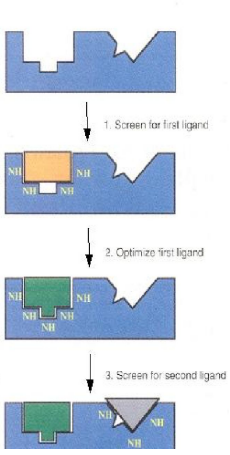


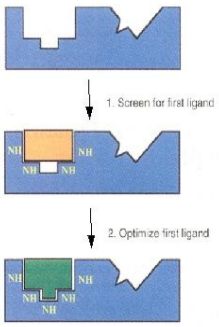


# SAR

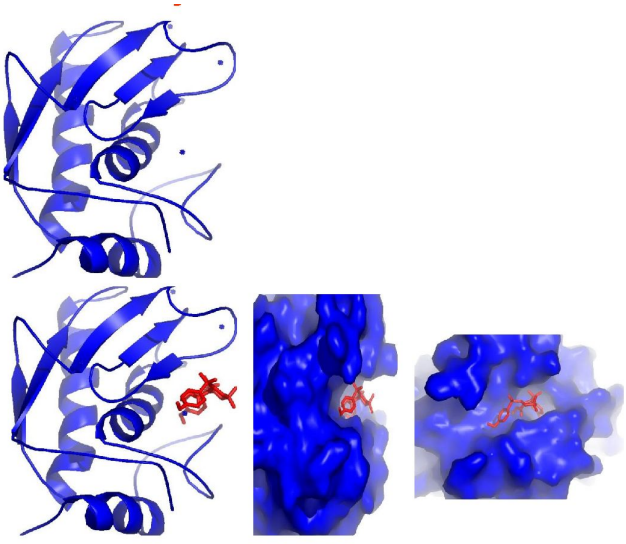

# SAR
# FBDD (fragment based drug design)

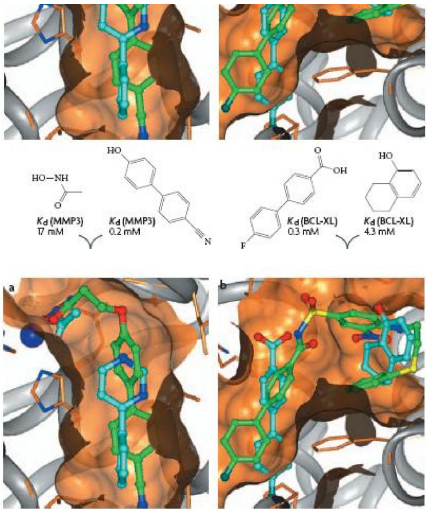


Identyfikacja fragmentów (K*d* mili do mikro mol).
Optymalizacja i wydłużanie.

# Twin-arginine translocation

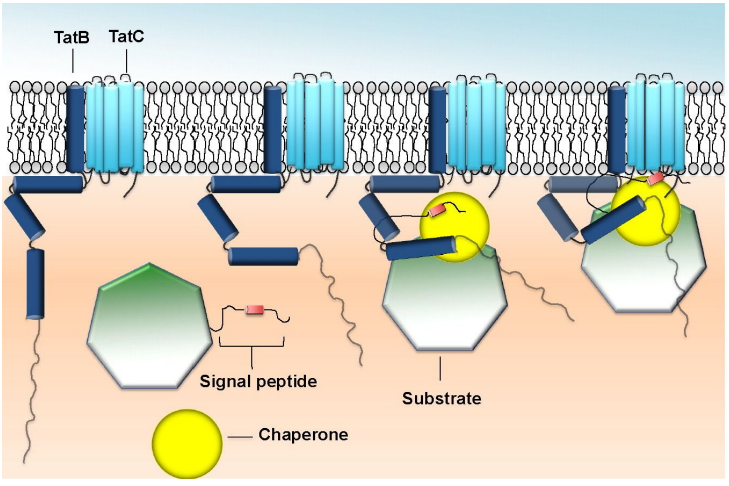

# Analiza konformacji lokalnych

**Oriented CD spectroscopy**

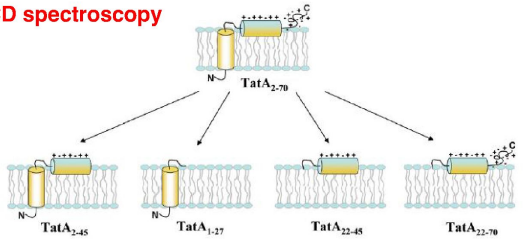


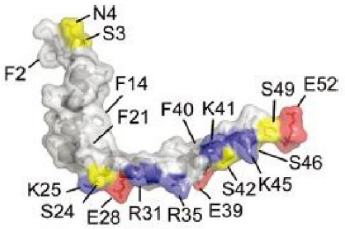


- TMH: fully buried
- N-terminal part of TMH (26-40): hydrophobic residues buried, hydrophilic residues partially exposed to water
- C-terminal part of TMH (41-48): mostly solvent exposed